学位論文

Analyses of the changes in stomatal and mesophyll CO_2 diffusion conductances in response to the atmospheric CO_2 concentration or soil water content

（気孔および葉肉における CO_2 拡散コンダクタンスの CO_2 濃度と土壌水分量への応答の解析）

平成２６年１２月　博士（理学）　申請

東京大学大学院理学系研究科

生物科学専攻

溝上　祐介

Abstract

CO_2 diffuses from ambient air to the chloroplast stroma. There are two large resistances in this diffusion pathway, stomatal resistance (r_s) and mesophyll resistance (r_m). r_s is the resistance from the leaf surface to the intercellular air space through stomata. r_m is the resistance from the intercellular air space to the chloroplast stroma. CO_2 concentration is highest in the air (C_a), and lowered in the intercellular air space (C_i) and lowest in the chloroplast stroma (C_c), because of substantial r_s and r_m. These resistances are often expressed as conductances, inverse of resistances, g_s and g_m.

These conductances respond to various environmental changes. In this thesis, I conducted detailed analyses of CO_2 diffusion conductances in response to drought and CO_2 concentration.

At first, I sought for factors that decrease g_m under drought conditions. ABA was one of candidates that would cause the decrease in g_m. Therefore, I used an ABA deficient mutant (*aba1*) and the wild type of *Nicotiana plumbaginifolia*. These plants were exposed to drought conditions to investigate whether the increase in ABA content in the leaves was needed for the decrease in g_m. For the g_m measurements, I constructed a special system to measure g_m with high accuracy using the carbon isotope method that is considered as most reliable. Under drought conditions, *aba1* did not show any decrease in g_m whereas g_m decreased in WT. Addition of ABA to *aba1* leaves caused dramatic decreases in g_m. I, thus, could demonstrate that the increase in ABA content in the leaf was necessary for the decrease in g_m. However, the underlying mechanisms are still not clear.

In addition to this experiment, I investigated whether g_m responded to high CO_2 condition with these tobacco plants because some papers have reported rapid decrease in g_m in response to high CO_2. In both WT and *aba1*, g_m decreased in response to high CO_2. Therefore, ABA might not be necessary for decrease in g_m in response to high CO_2.

There are only a few papers reporting detailed analyses of responses of g_m to elevated CO_2. In particular, studies reporting responses of g_m to long-tem elevation of CO_2 are few. Because, when the stomata close, Rubisco tends to fix more CO_2 evolved in the process of (photo)respiration than the CO_2 directly from the ambient air, I used some stomatal mutants of *Arabidopsis thaliana,* which are insensitive to CO_2, to uncouple the influence of g_s on g_m. To estimate g_m, I also applied new methods that were proposed very recently. The plants were grown at 390 ppm and 780 ppm in growth chambers to investigate whether the responses of g_m to elevated CO_2 could be changed by growth CO_2 concentration. In the short-term experiments, g_m decreased in response to elevated CO_2 regardless of g_s responses and the calculation methods to estimate g_m. In the long-term experiment, the responses of g_m to elevated CO_2 did not change with the growth CO_2 concentration. However, nitrogen nutrition during the growth affected responses of g_m to elevated CO_2. The difference might be due to changes in chloroplast starch metabolism. With the decrease in CO_2 concentration and/or nutritional N level, starch tended to accumulate, which would decrease g_m.

I investigated underlying mechanisms of the changes in g_m in response to elevated CO_2 and ABA. Recently, some studies have suggested that the PIP

aquaporins could affect g_m. Therefore, to clarify whether PIP aquaporins are involved in the changes in g_m in response to elevated CO_2 and ABA, I compared responses of g_m to elevated CO_2 and ABA among three T-DNA insertion lines of PIP aquaporins that are highly expressed in leaves (*pip1;2*, *pip2;3* and *pip2;6*). The responses of g_m to elevated CO_2 were all the same among Col-0 and all T-DNA insertion lines. However, in *pip2;6*, g_m was insensitive to ABA. As PIP2;6 was mainly expressed around the vascular tissue, PIP2;6 would not play roles in mesophyll cells as CO_2 facilitators. Previous reports have demonstrated that the relationships between leaf water relations and PIP aquaporins. Then the changes in the water relations would affect g_m.

Clarification of the relationships between leaf water relations and CO_2 diffusion in the leaves will be prerequisite to improve plant performance in semiarid and arid areas. Also, detailed analyses of responses of CO_2 diffusion conductances to high CO_2 will be helpful to improve plant performance in the high CO_2 world. The results are discussed in the light of these future perspectives.

Table of contents

Acknowledgements

I would like to express my appreciation to Professor Ichiro Terashima (The University of Tokyo), who gave me helpful and meaningful advice with excellent humor. I also thank Associate Professor Ko Noguchi (The University of Tokyo) for helpful advice and kind support.

I thank Dr. Annie Marion-Poll and Dr. Mitsunori Seo for providing the *aba1* and wild-type *Nicotiana plumbaginifolia* seeds.

I would thank Professor Ko Iba (Kyushu University) and Assistant Professor Juntaro Negi (Kyushu University) for providing the seed of *ost1* and *slac1-2,* and helpful discussion.

I would thank Associate Professor Munetaka Sugiyama (The University of Tokyo), Associate Professor Masaki Tateno (The University of Tokyo) and Associate Professor Kyoko Ohashi-Ito (The University of Tokyo) for examining my doctoral study and providing me valuable comments.

I would thank Associate Professor Izumi Mori (Okayama University) and Dr. Ayako Tsuchihira (Nagoya University) for kindly providing me PIP aquaporin T-DNA insertion lines.

I would like to express my appreciation to my family and friends for great support.

Finally, I would thank Emeritus Professor Haruko Kazama (International Christian University) for giving me special opportunity to be exposed to exciting science.

Abbreviations

C_a	CO_2 concentration in the air
C_{as}	CO_2 concentration at leaf surface
C_i	CO_2 concentration in intercellular air space
C_c	CO_2 concentration in chloroplast stroma
A	photosynthesis rate
a_b	carbon isotope discrimination caused by diffusion through boundary layer
a_s	carbon isotope discrimination caused by diffusion through stomata
a_i	carbon isotope discrimination during CO_2 diffusion/hydration through water
b	carbon isotope discrimination caused by the carboxylation reaction by Rubisco and phospho*enol*pyruvate carboxylase
e	the carbon isotope discrimination during day respiration
f	carbon isotope discrimination during photorespiration
R_d	day respiration
R_{dark}	dark respiration
Γ^*	CO_2 compensation point without the day respiration incorporated with g_m
C_i^*	CO_2 compensation point without the day respiration
Φ_{PSII}	Genty's parameter
SWC	soil water content
$[ABA]_L$	ABA contents of the leaves
g_s	stomatal conductance
g_m	mesophyll conductance
g_{lw}	total leaf stomatal conductance for H_2O
g_{cut}	cuticular conductance for H_2O
W_l	mole fraction of water vapor within the leaf
W_a	mole fraction of water vapor within the chamber air
E_l	total transpirastion rate
VPD	vapor pressure difference
Ψ_L	leaf water potential
S_c	surface area of chloroplasts facing the intercellular air space

S_m	surface area of mesophyll cells exposed to intercellular air space
PFD	photon flux density
LMA	leaf mass per unit area
AXS	artificial xylem sap

CHAPTER 1

General Introduction

Photosynthesis and CO_2 diffusion into the leaf

The substrate for photosynthesis, CO_2, diffuses from ambient air to the site of carboxylation, chloroplast stroma, along its concentration gradient, and is fixed by ribulose 1,5- bisphosphate carboxylase/oxygenase (Rubisco). There are three main resistances in this diffusion pathway, boundary layer resistance (r_b), stomatal resistance (r_s) and mesophyll resistance (r_m) (Fig. 1). r_b is the resistance to diffusion of gas in the leaf surface boundary layer that is formed through frictional interactions between the air and the leaf surface. r_b becomes greater when the air at the leaf surface is not stirred well. When photosynthetic measurements are made in gas exchange studies, r_b is often ignored because the air in the assimilation chamber is stirred very well. r_s is the resistance from the leaf surface to the intercellular air space through stomata. r_m is the resistance from the intercellular air space to the chloroplast stroma. CO_2 concentration is highest in the air (C_a), and is lower at the leaf surface (C_{as}) and further lowered in the intercellular air space (C_i) and lowest in the chloroplast stroma (C_c), because of r_b, r_s and r_m, respectively. These resistances are often expressed as conductances, inverse of resistances, g_b, g_s and g_m. Among these resistances, our knowledge of r_m is most scarce. Because r_m includes various partial resistances such as those of intercellular air space, cell wall, plasma membrane, cytosol, chloroplast envelope and chloroplast stroma, each of these partial resistances should be characterized. Although distance between the cell wall surface to the chloroplast stroma is shorter than that between leaf surface and the intercellular air space, CO_2 diffusion coefficient in liquid phase is about 1/10,000 of that in air, and thereby g_m and g_s are in the same order (Flexas *et al.*, 2008,

Terashima *et al.*, 2011).

Methodological advance to estimate mesophyll conductance

Early pioneering studies had suggested the resistance between the intercellular air space to chloroplast stroma could be a limiting factor for photosynthesis (Gaastra, 1959, Nobel, 1977). This was based on some morphological analyses. The leaves with high cumulated chloroplast surface areas facing the intercellular space per unit leaf surface area （chloroplast surface area, S_c）tended to show higher photosynthetic rates per leaf area. However, in many subsequent studies including those employing the photosynthesis model by Farquhar (Farquhar *et al.*, 1980), it was assumed that C_i was equal to C_c. Therefore, the decrease in the CO_2 concentration between the intercellular air space to chloroplast stroma have not been considered seriously.

Evans (1983) suggested the existence of mesophyll resistance based on gas exchange studies and biochemical analysis of Rubisco activity. There was a curvilinear relationship between the initial slope of photosynthesis rate-C_i curves (A-C_i curves) based on the Farquhar model, expressing the carboxylation efficiency, and the carboxylase activity of extracted Rubisco. The relation should be linear if C_i equals to C_c. Evans, thus, theoretically calculated g_m from the curvature.

g_m was estimated by Evans *et al.* (1986), by using the carbon isotope method, for the first time. This method was based on the characteristic of Rubisco; Rubisco discriminates $^{13}CO_2$ against $^{12}CO_2$. Rubisco fixes $^{12}CO_2$ in preference to$^{13}CO_2$ in the open system, whereas Rubisco fixes both $^{12}CO_2$ and $^{13}CO_2$ in the closed system. Plant

leaves are the intermediate semi-closed systems. Therefore, when conductivity of CO_2 to the chloroplast stroma is finite and low, the system becomes closer to the closed system and Rubisco tends to fix more $^{13}CO_2$. This characteristic makes it possible to quantitatively estimate conductivity in the leaf by measuring the ratio of $^{13}CO_2$ to $^{12}CO_2$ in the CO_2 fixed by photosynthesis. This carbon isotope discrimination model was also developed by Farquhar *et al.* (1989). Other methods to estimate g_m include the A-C_i curve fitting method and chlorophyll fluorescence method. The A-C_i curve fitting method was developed and improved by Ethier and Livingston (2004) and Sharkey *et al.* (2007). The chlorophyll fluorescence method was established by Harley *et al.* (1992). The latter involves simultaneous gas exchange measurements and chlorophyll fluorescence yield measurements. Because these two methods rely on models that have more assumptions than the carbon isotope models, the carbon isotope method is considered as the most reliable method to estimate g_m (Pons *et al.*, 2009).

There have been many studies that estimated g_m. However, almost all of them, in particular early field studies, employed the A-C_i curve fitting method or chlorophyll fluorescence method (Flexas *et al.*, 2008). Therefore, re-evaluation of their results is needed. Recently, the carbon isotope method has been also improved (Gu & Sun, 2014, Tholen *et al.*, 2012, Tholen & Zhu, 2011). The early models for the carbon isotope method do not incorporate the influence of respiration and photorespiration properly. Employing detailed simulations, Tholen and Zhu (2011) and Tholen *et al.* (2012) have claimed an emergent need for the incorporation of influenced of (photo)respiration. Gu and Sun (Gu & Sun, 2014) have also pointed out that the conventional carbon isotope

methods have misleading assumptions. It is necessary to use their methods for estimating g_m with data obtained from gas exchange and carbon isotope measurements.

Responses of g_m to environmental changes

It has been shown that drought, temperature, light intensity, vapor pressure deficit (VPD), nitrogen availability, salinity and CO_2 concentration alter g_m as reviewed in Flexas *et al.* (2008) and Flexas *et al.* (2012).

Under drought conditions, g_m and g_s decreased in many plant species in short-term experiments for minutes to hours as well as in long-term experiments for weeks to months scales (Delfine *et al.*, 2005, Flexas *et al.*, 2009, Flexas *et al.*, 2006a, Galmes *et al.*, 2007, Warren, 2008). Some of the reports have suggested that the decrease in g_m was recovered by re-watering (Flexas *et al.*, 2009, Galle *et al.*, 2009). These responses of g_m to drought have been well analyzed, however, underling mechanisms regulating g_m have not been clarified.

Responses of g_m to CO_2 concentration are still controversial. Short-term elevation of CO_2 tended to decrease g_m but marked decreases were not observed in wheat (Douthe *et al.*, 2011, Flexas *et al.*, 2007b, Tazoe *et al.*, 2009, Tazoe *et al.*, 2011). There are few reports for the plants grown in the elevated CO_2 for long terms and there appear to be no general trends (Bernacchi *et al.*, 2005, Singsaas *et al.*, 2004). Detailed analyses of g_m responses to CO_2 in both short-term and long-term scales are needed.

g_m variations in response to structural, physiological and molecular changes

Factors determining g_m are divided into two main categories, structural factors and biochemical factors. For structural factors, the diffusion pathway in the intercellular air space, cell wall thickness and chloroplast surface area exposed to the intercellular air space (S_c) would be important.

For evaluation of the resistance in the intercellular air space, A was measured in an artificial air, called helox, in which nitrogen is replaced with helium and compared with A measured in normal air. Diffusion coefficient of CO_2 in helox becomes 2.3 times greater than that in air. Parkhurst and Mott (1990) measured A in *Brassaia actinophylla*, and found that A measured in helox was greater than that measured in air. On the other hand, Genty *et al.* (1998) have reported that no difference was observed between A measured in helox and that in normal air in *Rosa rubiginosa* and *Populus koreana* × *trichocarpa*. In short, leaf structures differ from species to species. Therefore, the influence of intercellular diffusion pathway on g_m would be also different. Generally, in hypostomatous thick leaves, the resistance in the intercellular spaces could not be ignored, whereas in amphistomatous thin leaves commonly found in herbaceous plants, the intercellular resistance would be ignored.

CO_2 diffuses in the liquid phase in the cell wall. Therefore, cell wall thickness is an important factor to determine g_m. A previous study demonstrated that *Polygonum cuspidatum* from the site at 2500 m above sea level on Mt. Fuji had thicker cell wall and lower g_m compared to plants grown in the site at 10 m above sea level (Kogami *et al.*, 2001). g_m differs depending on plant functional types. g_m values are greatest in annual

herbs and decrease with the increase in cell wall thickness in perennial herbs, deciduous broadleaf trees and evergreen broadleaf trees in this order (Terashima *et al.*, 2006).

Early pioneering studies showed the importance of S_c for photosynthesis (Kariya, 1972, Laisk, 1970). Chloroplasts attach the cell membrane facing the intercellular air space when leaves are in the light. If chloroplasts are detached from the plasma membrane, CO_2 diffusion pathway might become greater and resistance becomes greater. Tholen *et al.* (2008) have demonstrated a positive relationships between S_c and g_m using a mutant of *Arabidopsis thaliana* that is impaired in chloroplast avoidance response. They also found that, in wild type plants, g_m and S_c changed simultaneously with translocational movement of chloroplasts in response to illumination of strong or weak blue light in a few minutes.

As biochemical factors, carbonic anhydrase (CA) and plasma membrane intrinsic protein (PIP) aquaporins have been considered as CO_2 facilitators in the liquid phase. CA could be divided into αCAs and βCAs, and βCAs are located near the plasma membrane, in cytosol, near the chloroplast envelope, in the stroma and in mitochondria in mesophyll cells (Fabre *et al.*, 2007). They catalyze hydration of CO_2 as follows, $CO_2 + H_2O \rightleftarrows HCO_3^- + H^+$, and this reaction is affected by pH. pH in the apoplast, cytosol and stroma is about 5.8, 7.4 and 8.0 under in high light, respectively (Terashima *et al.*, 2011). When CO_2 diffuses into cytosol or stroma, CO_2 is converted into HCO_3^-. When the pH values are 5.8, 7.4 and 8.0, $[HCO_3^-]$ / $[CO_2]$ ratios are 0.063, 15.8 and 63.1, respectively (Terashima *et al.*, 2011). HCO_3^- diffusion is slightly slower than CO_2 in

liquid phase, however, a concentration gradient of HCO_3^- is made in cytosol and stroma because of relatively high pH. In Price *et al.* (1994), antisense lines of a βCA, expressed in chloroplast, were made. However, they could not get clear results. Because there are six βCAs, further analyses are needed to investigate the relationships between CAs and g_m.

PIP aquaporins were reported as water channels. Thirteen species of PIPs have been identified in *Arabidopsis thaliana*, and they were further categorized into five PIP1s and eight PIP2s. Recently, it was shown that some PIP aquaporins serve as CO_2 channels, and antisense and overexpression lines of PIPs altered g_m (Flexas *et al.*, 2006b, Hanba *et al.*, 2004, Uehlein *et al.*, 2003). For water channel PIP aquaporins, regulation mechanisms via phosphorylation and protonation have been reported (Tornroth-Horsefield *et al.*, 2006, Van Wilder *et al.*, 2008). However, relationships between activity of PIP aquaporins and g_m have not reported yet. Therefore, it is important to analyze the activity of PIP aquaporins under various environmental conditions that could alter g_m.

Contents of this thesis

In CHAPTER 2, I investigated factors that decrease g_m under drought condition. Previous studies used chlorophyll fluorescence method for estimation of g_m to judge whether g_m decreases under drought conditions. However, the chlorophyll fluorescence method is not accurate. It is almost impossible to get all the parameters to estimate g_m especially in the field. Under drought conditions, it is difficult to use the carbon isotope

method for estimating g_m because drought stress often decreases the photosynthesis rate and thereby lowers the extent of discrimination for $^{13}CO_2$, which causes inaccuracy for estimating g_m. Herein, I constructed a special system to measure g_m with high accuracy, and measured whether ABA is involved in the decrease in g_m under drought conditions with mutants that impaired to produce ABA.

In CHAPTER 3, I investigated responses of g_m to CO_2 because there are only a few reports. In particular, studies reporting responses of g_m to long-tem elevation of CO_2 were few. Nevertheless, it is important to conduct such the study to predict the future photosynthetic production in the coming high CO_2 world. In addition to this, I used some mutants impaired in stomatal responses to CO_2 to uncouple the influence of g_s on g_m because changes in g_s affect the proportion of re-fixed CO_2 from (photo)respiration to the CO_2 directly from the ambient air. To exclude these uncertainties, I also applied new methods for estimation of g_m, which have been very recently proposed.

In CHAPTER 4, I investigated underlying mechanisms that change g_m in response to elevated CO_2 and ABA. Recently, some papers have suggested that the PIP aquaporins could affect g_m. Therefore, I assumed that the PIP aquaporins were one of the possible factors that regulate g_m in response to elevated CO_2 and ABA, and I investigated whether responses of g_m to elevated CO_2 and ABA were different among some T-DNA insertion lines of PIP aquaporins.

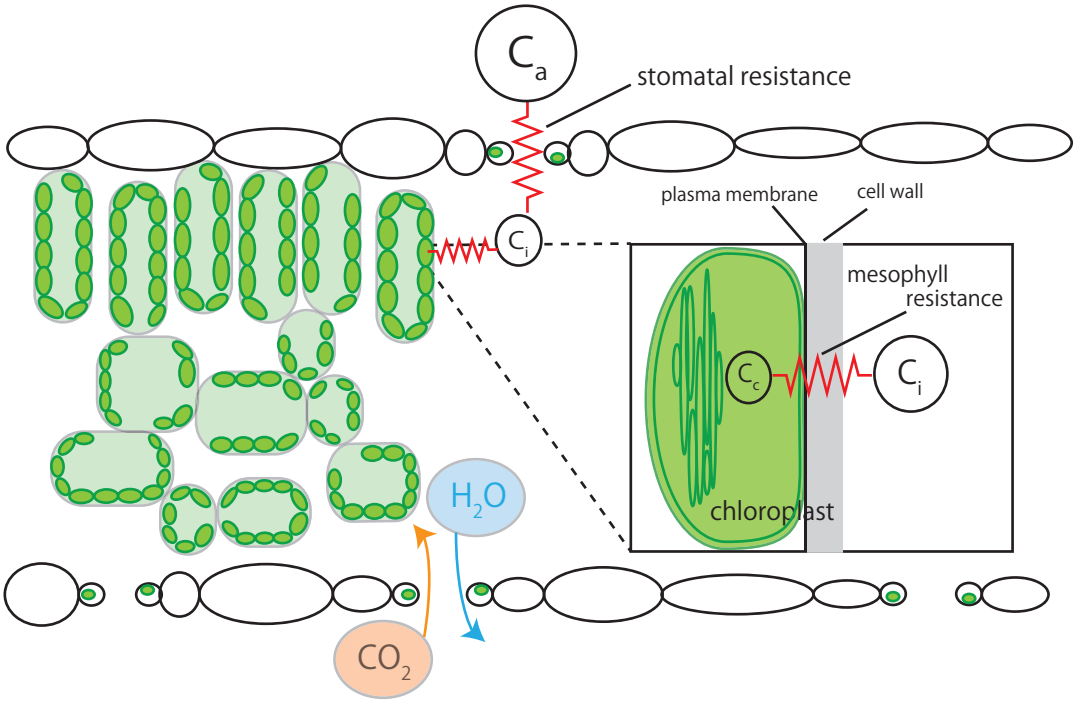

Fig. 1 CO_2 diffusion pathway in a leaf.

CHAPTER 2

Mesophyll conductance decreases in the wild type but not in an ABA-deficient mutant (*aba1*) of *Nicotiana plumbaginifolia* under drought conditions

Introduction

The balance between the H_2O efflux by transpiration and CO_2 influx from air to the chloroplast stroma is crucial for land plants. Excessive transpiration results in wilting, whereas low stomatal conductance limits CO_2 diffusion into the leaf and thereby photosynthesis. In particular, the drought stress disrupts the balance between H_2O efflux and CO_2 influx. Under drought conditions, CO_2 diffusion conductances through stomata (g_s) and from the intercellular air space to the site of carboxylation (g_m) decrease (Flexas *et al.*, 2009, Galmes *et al.*, 2007, Miyazawa *et al.*, 2008, Warren, 2008). The closure of stomata or the decrease in g_s under drought conditions has been studied well and it is established that ABA plays a crucial role (Ogunkanmi *et al.*, 1973, Tardieu *et al.*, 1992). In contrast, the mechanisms that decrease g_m is still unclear.

Three g_m measuring methods, namely, A-C_i curve-fitting, chlorophyll fluorescence/gas exchange and carbon isotope discrimination/gas exchange, have been used and the carbon isotope method is considered as the most reliable method with minimum assumptions (Pons *et al.*, 2009). However, estimation of g_m with the carbon isotope method under drought conditions is not feasible. Tholen *et al.* (2012) pointed out a serious influence of CO_2 produced by photorespiration on the calculation of g_m. Thus, measurements should be conducted at low oxygen concentrations to prevent the error in calculation of g_m. In most of the recent studies reporting the decreases in g_m under drought conditions, however, measurements of g_m were conducted at 21 % oxygen (Flexas *et al.*, 2009, Warren, 2008). Moreover, because the drought stress decreases the photosynthesis rate, the difference in the CO_2

concentration between the air entering the leaf chamber and the air leaving the leaf chamber decreases. The small difference in the CO_2 concentration causes inaccurate estimation of g_m (Caemmerer & Evans, 1991). Therefore, the use of reliable g_m measuring systems is needed to obtain accurate g_m under drought conditions. Moreover, under the drought conditions, leaf photosynthesis would be heterogeneous over the leaf area (Terashima, 1992). If the patchiness is marked, the conventional calculations will not be possible.

Abscisic acid (ABA) plays a major role in plant responses to drought stress (Shinozaki & Yamaguchi-Shinozaki, 2007). Recently, the rapid production of ABA in xylem parenchyma cells has been reported and involvement of ABA transporters in the export of ABA from ABA-producing cells has been also suggested (Christmann *et al.*, 2007, Endo *et al.*, 2008, Kuromori *et al.*, 2010). Stomatal closure is one of the responses mediated by ABA. For g_m, Flexas *et al.* (2006a) also showed that ABA application to soybean and tobacco decreased g_m, although these measurements were conducted by the chlorophyll fluorescence/gas exchange method. Long-term drought treatments of tobacco plants for two to three weeks decreased g_m (Miyazawa *et al.*, 2008). However, the long-term drought treatments might induce acclimation including changes in leaf anatomical traits. Such acclimation would complicate the relationships between the decrease in g_m under drought condition and the involvement of ABA. In *Helianthus annuus*, g_s measured three days after the application of a 20 μM ABA solution to the roots decreased considerably, whereas g_m was unchanged (Vrabl *et al.*, 2009). In the study by Vrabl *et al.* (2009), it could be possible that leaf ABA level was not

enough to decrease g_m but enough to decrease g_s.

The aim of this study was to investigate whether ABA is involved in decreasing g_m under relatively short-term drought stress. We used the wild type and an ABA deficient mutant of *Nicotiana plumbaginifolia* and measured g_m with a custom-made system at a low O_2 concentration of 1%.

Materials and methods

Plant materials and growth conditions

The wild type and an ABA deficient mutant (*aba1*) of *Nicotiana plumbaginifolia* were grown in 900 mL pots containing river sand (Suna, SOSEKI, Tochigi, Japan) in a growth chamber with a 14 h photoperiod, day/night temperature of 23/21°C and at relative humidity of 70%. Light was provided by a bank of white fluorescent lamps (FPR-96EXNA, National, Osaka, Japan) and the photon flux density (PFD) at the plant level was 400 μmol m^{-2} s^{-1}. The river sand was completely oven-dried at 80°C and 1 kg of dried river sand was used per one pot. Plants were irrigated two to three times a week with the 1/1000 strength solution of a commercial nutrient solution (Hyponex 6-10-5; Hyponex Japan, Osaka, Japan), containing 6.00% total nitrogen, 10.0% water-soluble phosphoric acid and 5.0% water-soluble potassium. *aba1* is the mutant that hardly produce ABA because *aba1* lacks an activity of aldehyde oxidase (AO) that catalyzes a oxidation of abscisic aldehyde to ABA (Seo & Koshiba, 2002).

Drought treatment and ABA application

For the drought treatment, irrigation was withheld. As an indicator of drought stress, we used soil water content (SWC) calculated as:

$$SWC(\%) = \frac{W - W_D}{W_{FC} - W_D},$$

where W is the soil weight at the time point of the measurement, W_D is the soil dry weight after oven-dried at 80°C for three days , W_{FC} is the soil weight at the field capacity. In this study, field capacity is defined as the wet weight measured after gravity water was drained in 20 min. The drought treatment was applied when the 12th to 14th leaves of 8 weeks-old plants were fully expanded. Measurements of photosynthetic parameters were conducted when SWC was 100% and 40 ± 4%. Both WT and *aba1* wilted at SWC less than about 35% (data not shown).

ABA was applied to a detached leaf. The plant was kept in the dark for 30 min and the leaf was cut at its petiole base under deionized water. The petiole of the detached leaf was kept in the deionized water in a 1.5 mL micro tube. Then the deionized water in the micro tube was replaced with an artificial xylem sap (AXS) containing 1 mM potassium phosphate buffer(pH 5.8), 1 mM $CaCl_2$, 0.1 mM $MgSO_4$, 3 mM KNO_3 and 0.1 mM $MnSO_4$ (Wilkinson & Davies, 1997). The detached leaf was enclosed in the leaf chamber (for the conditions, see below) and gas exchange measurements were conducted after photosynthesis became stable about 2 h after the petiole cutting. The AXS in the micro tube was then replaced with an AXS containing 1 μM or 10 μM ABA. When steady-state leaf photosynthesis was attained, gas exchange measurements

were conducted.

Gas exchange and isotopic measurements

Gas exchange measurements were performed with a laboratory-made chamber and an infrared gas analyzer system (LI-7000; Li-Cor, Inc., Lincoln, NE, USA). The chamber size was 100 × 80 × 20 mm with two DC fans to obtain a large boundary layer conductance. For the measurements of *N. plumbaginifolia* leaves, the fully expanded leaf was enclosed in the chamber. Light at PFD of 800 μmol m^{-2} s^{-1} was provided by a metal halide lamp (PCS-UMX250; NPI, Tokyo, Japan). The rate of photosynthesis was measured at an ambient CO_2 concentration (C_a) of 390 μmol mol^{-1} and O_2 concentration of 1% to minimize the effect of photorespiration. To correct the O_2 effect on sensitivity of infrared CO_2/H_2O analyzer, I used the LI-6400 built-in correction formulae (Bunce, 2002). The leaf temperature was kept at 25°C and the leaf to air vapor pressure deficit (VPD) was set to 0.9 – 1.0 kPa. Gas exchange parameters were calculated according to von Caemmerer & Farquhar (1981). When leaf photosynthesis reached its steady-state rate, the air leaving the LI-7000 from reference and sample cells were captured in the 100 ml Pyrex^{TM} bottles for three times each. The ratio of $^{13}CO_2$ to $^{12}CO_2$ in the air in the Pyrex bottles was analyzed with a mass spectrometer (IsoPrime 100; Isoprime Ltd, Manchester, UK) equipped with a CO_2 concentration system (trace gas system). The accuracy of this $\delta^{13}C$ measurement system was less than ± 0.06‰ of standard deviation (n= 5, data not shown). Carbon isotope ratio was expressed as $\delta^{13}C$ calculated as

$$\delta^{13}C = \frac{R_{air}}{R_{standard}} - 1$$

where R_{air} and $R_{standard}$ are the carbon isotope ratios of the air leaving the LI-7000 and the standard, PeeDee belemnite, respectively.

Carbon isotope discrimination (Δ) was calculated according to Evans *et al.* (1986) as:

$$\Delta = \frac{1000 \times \xi\left(\delta^{13}C_{sam} - \delta^{13}C_{ref}\right)}{1000 + \delta^{13}C_{sam} - \xi\left(\delta^{13}C_{sam} - \delta^{13}C_{ref}\right)},$$

where $\xi = C_{ref}/\left(C_{ref} - C_{sam}\right)$ and C_{ref} and C_{sam} are the CO_2 concentrations of the air entering and leaving the chamber, respectively, analyzed with LI-7000. In all measurements, ξ values were was set to less than 10 to keep the accuracy of g_m calculation high.

A - C_i curves were obtained by measuring A at C_a of 100, 200, 390, 600, 800 and 1000 μmol mol^{-1} and g_m values were also calculated at all these C_a concentrations.

Calculation of mesophyll conductance

The calculation of mesophyll conductance was based on Tazoe *et al.* (2011). However, I did not ignore boundary layer conductance though it was high enough. Discrimination of CO_2 during C_3 photosynthesis is expressed according to Evans *et al.* (1986):

$$\Delta = a_b \frac{C_a - C_{as}}{C_a} + a_s \frac{C_{as} - C_i}{C_a} + a_i \frac{C_i - C_c}{C_a} + b \frac{C_c}{C_a} - \frac{eR_d/k + f\Gamma^*}{C_a},$$

where C_a is the ambient CO_2 concentration, C_{as} is the CO_2 at the leaf surface, C_i is the intercellular CO_2, C_c is the CO_2 at the chloroplast stroma. These CO_2 concentration is calculated from Fick's first law (e.g. $A=g_b(C_a - C_{as})$). a_b and a_s is the carbon isotope discrimination caused by diffusion through boundary layer (2.9‰) and stomata (4.4‰), respectively, a_i is the carbon isotope discrimination during CO_2 diffusion/hydration through water (1.8‰), and b is the carbon isotope discrimination caused by the carboxylation reaction by Rubisco and phospho*enol*pyruvate carboxylase (30‰). e is the carbon isotope discrimination during day respiration, and I assumed no fractionation by the day respiration and calculated it based on Tazoe *et al.* (2009) as follows:

$e=\delta^{13}C_{\text{gas cylinder}} - \delta^{13}C_{\text{atmosphere}}$.

In this study, the carbon isotope composition in the chamber air provided with CO_2 gas cylinder, $\delta^{13}C_{\text{gas cylinder}}$ was -34.36‰ and the carbon isotope composition in the growth chamber, $\delta^{13}C_{\text{atmosphere}}$, was assumed to -13.56‰, the average value of five replicates. Therefore, e was set to -20.8‰. Day respiration (R_d) is assumed to be the same as the dark respiration (R_{dark}). The symbols f (11.6‰) and Γ^* are the carbon isotope discrimination during photorespiration and a CO_2 compensation point without the day respiration, respectively (Lanigan *et al.*, 2008). Γ^* was assumed to be 1.468 μmol mol^{-1} under 1% O_2 based on the actual data obtained in this study using the Laisk method (Laisk, 1977). The symbol k is the carboxylation efficiency of Rubisco and $k= V_c/C_c$ where $V_c= (A + R_d)/(1 - \Gamma^*/C_c)$ (Tazoe *et al.*, 2011, Von Caemmerer & Farquhar, 1981). C_c is calculated from Fick's first law, $A=g_m(C_i - C_c)$.

Mesophyll conductance was calculated according to Tazoe *et al.* (2011) as

$$g_m = \frac{\left(b - a_i - \frac{eR_d}{A + R_d}\right)\frac{A}{C_a}}{a_b + (a_s - a_b)\frac{C_{as}}{C_a} + (b - a_s)\frac{C_i}{C_a} - \frac{eR_d(C_i - \Gamma^*)}{C_a(A + R_d)} - \frac{f\Gamma^*}{C_a} - \Delta}.$$

Measurement of ABA content in the leaf, Rubisco content and leaf water potential

For measuring the ABA content, 4 to 6 leaf discs (50 – 100 mg) per leaf were obtained avoiding the midribs with a leaf punch right after the measurements of photosynthetic characteristics in the leaves of well-watered plants, water stressed plants and those fed with ABA. The samples were stored in a freezer at –80°C. The ABA content was analyzed with an ultra-performance liquid chromatography (UPLC) coupled with a tandem quadrupole mass spectrometer (qMS/MS) equipped with an electrospray interface (ESI; UPLC-ESI-qMS/MS) (Kojima *et al.*, 2009).

For measuring the Rubisco content, leaf discs were taken from the leaves at SWC of 100% or 40 ± 4%. The Rubisco content was measured according to Makino *et al.* (1986) with some modifications. Leaf discs were homogenized in a 62.5 mM Tris-HCl buffer (pH 6.8) containing 7.5% (v/v) glycerol, 5 mM DTT, 2% SDS and the protease inhibitor cocktail (Roche Diagnostics K.K., Tokyo, Japan) and then boiled at 95°C for 5 min. The sample was centrifuged at 20,000 *g* for 10 min and the supernatant was used for SDS-PAGE. SDS gels were stained with Coomassie Brilliant Blue for two hours with gentle shaking and then de-stained with 30% (v/v) methanol containing 10% (v/v) acetic acid until the gel background getting clear. The bands considered as Rubisco large subunits were taken out with a razor blade and extracted with formamide for 5 h. The

extraction was analyzed with a spectrophotometer (UV 3310, HITACHI, Tokyo, Japan) and the Rubisco content was determined. I used bovine serum albumin as the standard.

Two hours after the clamping the leaf in the chamber under the same conditions as those for g_m measurements, leaf water potential was measured with a pressure chamber (Model-3000, SoilMoisture Equipment Corp., Santa Barbara, CA, USA) .

Non-uniform stomatal closure by abscisic acid

The detached leaf with its petiole kept in a micro tube containing the AXS was enclosed in a 6 cm^2 chamber of a portable gas exchange system (LI-6400; Li-Cor) and placed under a 2-D fluorescence imaging system (FluorCam, Photon System Instruments Ltd, Brno, Czech Republic). In the chamber, CO_2 and O_2 concentration were kept at 390 μmol mol^{-1} and 1 %. The LEDs of the 2-D FluorCam gave 400 μmol m^{-2} s^{-1}at the leaf surface. The leaf temperature and VPD were kept at 25°C and at 0.8 – 1.0 kPa respectively. The ABA concentration in the AXS was increased stepwise to 100 μM after the steady-state leaf photosynthesis was attained at each ABA concentration.

To validate the effects of the ABA application on the uniformity of leaf photosynthesis, I analyzed photosystem II quantum yields (Genty's parameter:Φ_{PSII}) over the leaf before and after the ABA application. Φ_{PSII} was calculated using the following equation by Genty *et al.* (1989):

$$\Phi_{PSII} = \frac{(F_m' - F_s')}{F_m'}$$

where F'_s is a steady-state fluorescence and F'_m is a maximal fluorescence during a light-saturating pulse in the presence of actinic light.

Results

Photosynthetic parameters and ABA content in leaves

To investigate possible involvement of ABA in decreasing g_m under drought conditions, I used an ABA deficient mutant, *aba1*, and photosynthetic characteristics of this mutant and the wild type were compared. The rate of decrease in SWC after withholding irrigation was faster in *aba1* than WT (Fig. 1). This would be due to the greater transpiration rate in the *aba1* plants as has been suggested (Leydecker *et al.*, 1995).

The photosynthetic parameters of WT and *aba1* are shown in Fig. 2. At SWC 100 %, g_s was somewhat greater in *aba1* than in WT. On the other hand, g_m values were almost the same. In WT, both g_s and g_m were lower at SWC 40 ± 4% than at the SWC 100%. On the other hand, neither g_s nor g_m decreased in *aba1* (Fig. 2). I also examined the ABA contents of the leaves ($[ABA]_L$) under both well-watered and drought conditions. $[ABA]_L$ increased by more than tenfold under the drought condition in WT. However, in *aba1*, $[ABA]_L$ did not increase but remained at a low level even under the drought condition (Fig. 3). Although $[ABA]_L$ under the drought condition was somewhat dispersed in WT, a strong correlation can be seen when the data of g_m and $[ABA]_L$ were plotted (Fig. 5).

To validate the effect of ABA on g_m, I artificially changed the $[ABA]_L$ by feeding ABA. Both g_s and g_m decreased when the leaves of WT and *aba1* were fed with ABA via their petioles. The decreases in photosynthetic parameters by ABA were in a dose-dependent manner in both WT and *aba1* (Fig. 4).

g_s and g_m were negatively correlated with $[ABA]_L$ in both WT and *aba1*, when the data of the drought experiments (Fig. 2 and 3) and the ABA feeding experiments (Fig. 4) were plotted together (Fig. 5). It is noteworthy that g_s was more sensitive to $[ABA]_L$ than g_m. A was correlated with both g_s and g_m in both WT and *aba1* (Fig. 6). Because the decrease in A was clearly due to limitation of CO_2 diffusion conductance in the leaves, and because g_s and g_m were suppressed by ABA, $[ABA]_L$ is clearly a major determinant of A under the drought conditions.

Analyses at different C_a levels showed that g_s and g_m decreased with the increase in C_i in both WT and *aba1* (Fig. 7). g_s was greater in *aba1* than in WT. However, g_m levels were smaller in *aba1* than in WT at the low C_i range (< C_a: 390 μmol mol^{-1}). g_m levels were almost the same at higher ranges. The data of the ABA feeding experiments were superimposed. It is worth noting that the ABA feeding and exposure to low CO_2 caused the inverse responses of g_m, although both treatments caused the decreases in C_i. Accordingly, A-C_i relationships also changed, because g_m decreased in the presence of ABA. g_s values in the control leaves of the ABA feeding experiments were somewhat greater than those in the leaves used for CO_2 responses probably because I used the cut leaves in the ABA feeding experiment.

Leaf Rubisco content and leaf water potential

The leaf Rubisco contents were not different between the well-watered (0.913 ± 0.180 g m^{-2}) and drought conditions (0.9138 ± 0.187 g m^{-2}) in WT. Leaf Rubisco content of *aba1* did not significantly change between the well-watered (0.878 ± 0.073 g m^{-2}) and drought conditions (1.027 ± 0.125 g m^{-2}), either. Therefore, neither the changes in A nor those in g_m were explained by the changes in the Rubisco contents.

The leaf water potential (Ψ_L) in WT decreased after the drought treatment (Fig. 8). However, Ψ_L were not different between SWC 100% and 40 ± 4% in *aba1*. It was also noted that *aba1* showed lower Ψ_L than WT even under the well-watered conditions.

When fed with 100 μM ABA, Φ_{PSII} decreased uniformly over the leaf area (supplementary data. 1). Heterogeneity in Φ_{PSII} over the leaf area was not detected in the leaves even at SWC of 40% (supplementary data. 2). Because the leaf area enclosed in the assimilation chamber was about 15 cm^2 and was not much greater than the area (6 cm^2) tested for uniformity of photosynthesis, under the present experimental conditions, patchy stomatal closure might not occur.

Discussion

It has been reported for many species that both of the CO_2 diffusion conductances, g_s and g_m, decrease under drought conditions (Flexas *et al.*, 2006a, Flexas *et al.*, 2008, Galmes *et al.*, 2007). Further, Flexas *et al.* (2006a) argued that ABA could decrease not only g_s but also g_m. However, few relationships between the decrease in g_m and the $[ABA]_L$ have been reported. The responses of g_m to ABA so far reported were not

consistent. This is partly because the g_m measuring method, the ABA concentration applied, and/or the period of ABA treatment, vary depending on the studies (Flexas *et al.*, 2006a, Vrabl *et al.*, 2009). Under prolonged drought conditions, g_m may acclimate to the conditions and recover towards the original level (Flexas *et al.*, 2009). Therefore, I focused on the responses of g_m to drought stress and the involvement of ABA in these responses in the relatively short period up to three days.

Involvement of ABA under drought conditions prevents excessive water loss by inducing several plant responses including closure of stomata through ABA signaling cascades (Shinozaki & Yamaguchi-Shinozaki, 2007). *aba1* hardly produces ABA even under drought condition because of the defect in generating the sulfurylated form of the molybdenum cofactor that is necessary for the activity of the aldehyde oxidase (AO). AO catalyzes the main pathway for oxidation of ABA aldehyde to ABA in the cytosol. There are some other pathways to produce ABA like the abscisic alcohol pathway. Thus, ABA production in *aba1* is not null (Seo & Koshiba, 2002). In the present study, the ABA content in the *aba1* leaves at SWC of 40 ± 4% was similar to that at SWC of 100%. The rate of the decrease in SWC was faster in *aba1* than in WT, because the stomata in *aba1* were kept widely open even under drought conditions (Fig. 2). The use of the ABA deficient mutant *aba1* was effective for investigating the relationship between ABA content in the leaves and decrease in g_m under drought conditions.

Some reports indicate that soil water deficit decreases g_s and g_m similarly (Flexas *et al.*, 2008, Warren, 2008). However, there are only a few reports taking full account of the accuracy of the g_m measurements under low g_s condition. Because Tholen *et al.*

(2012) indicated that respiration and photorespiration interfere with the measurement of g_m obtained under at 21% O_2 , in the present study, all g_m measurements were conducted at 1% O_2. I also checked that the patchy stomatal closure was unlikely even under the severest conditions adopted in the present study. Moreover, I evaluated the effect of cuticular conductance on C_i calculation according to Boyer *et al.* (1997). When WT leaves were fed with 10μM ABA, g_s for H_2O decreased to about 0.1 mol H_2O m^{-2} s^{-1} (see Fig. 4, but in this figure g_s values for CO_2 are shown). If cuticular conductance is 1, 5 or 10 mmol H_2O m^{-2} s^{-1}, C_i will be about 195.32±18.6, 187.82±21.0 or 177.34±25.1 μmol CO_2 mol^{-1} respectively (cf. C_i with no cuticular transpiration, 197.09±18.05 μmol CO_2 mol^{-1}), and g_m will be 0.095±0.009, 0.102±0.013 or 0.115±0.023 mol CO_2 m^{-2} s^{-1} respectively (cf. g_m with no cuticular transpiration, 0.094±0.009 mol CO_2 m^{-2} s^{-1}). I did not measure the cuticular conductance in this study but from the above calculations I would be able to confirm that the decrease in g_m values by ABA were mostly attributed to the decrease in g_m per se (for details, see Appendix). In WT, g_m was decreased with the increase in $[ABA]_L$ under the drought conditions. When the data from the drought experiments and the ABA feeding experiments were plotted together, a strong tendency that g_m decreased with the increase in $[ABA]_L$ was evident (Fig. 5). Therefore, I conclude that g_m was decreased by ABA in a dose-dependent manner and that g_m did not decrease even under the drought condition in *aba1* because of the very low level of ABA.

When treated with 10 μM ABA, g_m was decreased to the about half that in the control (Fig. 4). Terashima *et al.* (2011) suggested that the cell wall resistance account

for about half of the mesophyll resistance in annual herbs. The cell wall thickness should not be altered in about two hours, therefore ABA would somehow affect the membranes. However, I have to consider the effects of cell walls in a careful way because pH in the xylem sap and the apoplastic space may increase under drought conditions (Wilkinson & Davies, 1997). Terashima *et al.* (2011) also pointed out that the porosity and tortuosity of the cell wall could be changed with pH. In the present study, I did not change pH of the AXS; all the ABA application experiments were conducted using the AXS of pH 5.8. When I switched AXS pH from 5.8 to 7.0, the tobacco leaves wilted (data not shown). I can see some differences in the conductance data between the drought experiments and those using 1 μM ABA though $[ABA]_L$ were in the same range (Fig. 5). Effects of pH on g_m and g_s should be studied.

In *N. plumbaginifolia* leaves that were fed with ABA, g_s was more significantly limiting photosynthesis than g_m (Fig. 5). Most notably, this is the first study to our knowledge to simultaneously investigate the effects of ABA on g_s and g_m using the ABA deficient mutants. This kind of approach may clarify the evolutionary scenario of acquisition of ABA responsiveness of g_s and g_m. For example, in some ferns, stomatal closure in response to water stress is not due to ABA (McAdam & Brodribb, 2012). Whether g_m in ferns responds to ABA remains unknown.

The decreases in both g_s and g_m under drought conditions shown would be free from the artifact due to (photo)respiration, which was pointed out by Tholen *et al.* (2012) because all the measurements were conducted at 1% O_2. The simultaneous decreases of g_s and g_m might be partly due to the secondary effect of changes in leaf hydraulics.

This possibility, the relationship between g_m and the leaf hydraulics, has been claimed by Ferrio *et al.* (2012). In the present study, Ψ_L was decreased in WT after the drought treatment (Fig. 8). The decrease in Ψ_L might have been associated with deactivation of aquaporins in bundle-sheath cells because Shatil-Cohen *et al.* (2011) reported that application of ABA caused the deactivation of aquaporins and then decrease in Ψ_L. Activities of the plasma membrane intrinsic proteins (PIPs) are regulated by various ways; phosphorylation, protonation and internalization (localization change) (Boursiac *et al.*, 2008, Tornroth-Horsefield *et al.*, 2006, Tournaire-Roux *et al.*, 2003a). In the present study, especially in the ABA feeding experiments, the activities of PIPs might be regulated by these mechanisms because the decrease in g_m occurred within a short time of less than 30 mins. Prak *et al.* (2008) showed a possibility that the *At*PIP phosphorylation state is crucial for the subcellular localization of the PIPs in *Arabidopsis thaliana*. In addition to this, a decrease in the apoplastic water potential of maize seedlings resulted in the decrease in phosphorylation state of *Zm*PIP (Van Wilder *et al.*, 2008). These studies on the PIP activation state under abiotic stresses have been conducted with the roots. Therefore, I have to conduct similar studies with leaves focusing on the mesophyll cells. The decrease in Ψ_L could induce shrinkage of mesophyll cells as reported in Canny *et al.* (2012). This could be one candidate responsible for the short-term response of g_m because the shrinkage of mesophyll cells would induce decrease in S_c.

The duration of the ABA- and/or drought treatments, the dose of ABA, and/or plant species might bring about different results. For example, the long-term drought

treatments decreased g_m in tobacco whereas the long term ABA feeding treatment did not change g_m but decreased g_s in *Helianthus annuus* (Miyazawa *et al.*, 2008, Vrabl *et al.*, 2009). This difference in the responses might be dependent on growth strategies of the plants. In the case of Vrabl *et al.* (2009), it might be possible that the leaf ABA level was not enough to decrease g_m but enough to decrease g_s. Our results showed that g_s was more sensitive to $[ABA]_L$ than g_m. These differences in the ABA sensitivity could explain the different behaviors of g_s and g_m in responses to vapor pressure difference (VPD). Warren (2008) pointed out that both g_s and g_m decreased following the decrease in the soil water content, but only g_s decreased in response to the increase in VPD. The response of g_s to VPD has been considered as an ABA independent response (Assmann *et al.*, 2000). However, very recently, Bauer *et al.* (2013) suggested that the response of the guard cells to low relative humidity occurred in an ABA dependent manner. The $[ABA]_L$ must be very low when g_s responds to the increase in VPD, because this response is too rapid for appreciable ABA production. These results indicate that the slight increase in the leaf ABA level is enough to decrease g_s but not to decrease g_m. In addition, the ABA level around stomata might get higher because ABA in the mesophyll cells (in the apoplast) moves to stomata by mass flow and becomes concentrated at the evaporation sites around the stomata.

As shown in Fig. 7, g_s and g_m responded to changes in CO_2 in both WT and *aba1*. The responses of g_s to CO_2 have been reported and reviewed (Ainsworth & Long, 2005, Ainsworth & Rogers, 2007, Bunce, 1998). Our results suggested ABA is not necessarily important for response of g_s to CO_2, although *aba1* showed higher g_s than WT

throughout all the CO_2 range. On the other hand, the responses of g_m to CO_2 are controversial. Flexas *et al.* (2007a) evaluated six different C_3 species and showed responses of g_m to CO_2. Tazoe *et al.* (2009) also examined CO_2 responses of g_m in wheat. In wheat, however, g_m did not vary much with CO_2. In the present study, g_m varied with CO_2 in a few minutes as already reported in Tazoe *et al.* (2011) for Tobacco, *A. thaliana* and wheat and the CO_2 response was faster than the ABA response. The response of g_m to CO_2 in *aba1* suggested that ABA should be unnecessary for the decrease in g_m, although further conclusive investigations are still needed. The fast changes in g_m with CO_2 might be due to the involvement of carbonic anhydrase (CA). CA catalyzes the interconversion of $CO_2 + H_2O \Leftrightarrow HCO_3^- + H^+$ quickly. In *A. thaliana*, 14 CAs (five αCAs and eight ßCAs) have been characterized and ßCA4 was localized near the plasma membrane (Fabre *et al.*, 2007). CO_2 that enters the cytosol of mesophyll cells is associated with H_2O and rapidly converted to $HCO_3^- + H^+$ by ßCA4 or other CAs. The local concentration of H^+ on the plasma membrane of the cytosolic side is thus increased and thereby the local pH decreases. According to Tournaire-Roux *et al*. (2003), the decrease in cytosolic pH by 1.0 caused inhibition of root water transport activity. The local pH decline near the plasma membrane in the mesophyll cells might induce deactivation of PIPs.

Another interesting point was that the decrease in g_m in *aba1* was less than that in WT at low CO_2 levels. To explain the differences in the g_m responses between WT and *aba1*, I have to consider acclimation because in these plants g_s and Ψ_L were different. The higher g_s in *aba1* resulted in the higher C_i by about 20 μmol mol^{-1} at C_a of 390 μmol

mol^{-1}. This difference in C_i might not influence the expression levels of CAs especially ßCAs because there was no difference in mRNA expression levels of ßCAs irrespective of the growth C_a levels at 150 µmol mol^{-1} and 1000 µmol mol^{-1} (Fabre *et al.*, 2007). On the other hand, Ψ_L in *aba1* was low even at 100% SWC (Fig. 10). The low Ψ_L would be an ABA-independent water stress signal that induces some acclimation, which might play a role in decreasing g_m at low C_i levels in *aba1*. I need further analyses of the relationships between Ψ_L and the g_m response to CO_2. In this study, I measured responses of g_m to ABA and CO_2. I plotted these data together in Fig. 7. There were the different trends of A in responses to C_i because responses of g_s and g_m were different between ABA and low CO_2 treatments, though both treatments induced low C_i. These different responses strongly indicate that the regulation mechanisms of g_m in response to ABA and CO_2 are different. The differences in the A-C_i relationships are also important. The decrease in A at a given C_i in the ABA treated leaves would be mostly explained by the decrease in g_m, although a small part of the decrease could be attributed to the overestimation of C_i due to the neglection of cuticular conductance. The conclusion of the studies that examined the stomatal patchiness problems (Downton *et al*. 1988, Terashima *et al.* 1988, Terashima *et al*. 1992) was that the depression in A at a given C_i in the ABA treated leaves or in water-stressed leaves was attributed to overestimation of C_i due to patchy stomatal closure over the leaf area. However, this view would be too simplistic, because ABA certainly decreases g_m at least in the present material.

Both of the drought experiment and ABA feeding experiments in the present study

clearly showed the negative relationship between $[ABA]_L$ and g_m. In addition, possible involvement of leaf hydraulics on g_m regulation is suggested in both the ABA response and CO_2 response. To figure out the mechanisms of ABA responses of g_m, future works should focus on the effects of aquaporin activity on leaf hydraulics and g_m because the leaf is an important point of intersection of CO_2 and H_2O fluxes.

Appendix: Estimation of C_i considering the cuticular conductance

In this appendix I express the leaf conductance (stomatal + cuticular conductance) for H_2O as g_{lw}. The relative contribution of the cuticular conductance to g_{lw} increase with decreasing g_{lw} and the overestimation of C_i would occur because the cuticular conductance for H_2O is far much greater than that for CO_2. I estimated C_i considering cuticular conductance at low g_s:

$$C_i = \frac{(g_{sc} - E_s/2)C_{as} - A}{g_{sc} + E_s/2}$$

where C_{as} is the CO_2 concentration at the leaf surface, A is the photosynthesis rate, g_{sc} and E_s are the true stomatal conductance for CO_2 and true stomatal transpiration rate considering the cuticular transpiration (Boyer *et al*. 1997). g_{sc} and E_s are expressed as:

$$g_{sc} = (g_{lw} - g_{cut})/1.6$$

$$E_s = E_l - g_{cut}(W_l - W_a)$$

where g_{lw} is the total leaf stomatal conductance for H_2O, E_l is the total transpirastion rate, g_{cut} is the cuticular conductance for H_2O, and W_l and W_a are the mole fraction of water vapor within the leaf and that in the chamber air. I assumed g_{cut} of 1,5 or 10 mmol H_2O mol m^{-2} s^{-1} and calculated C_i and g_m for the WT leaves fed with 10 μM ABA.

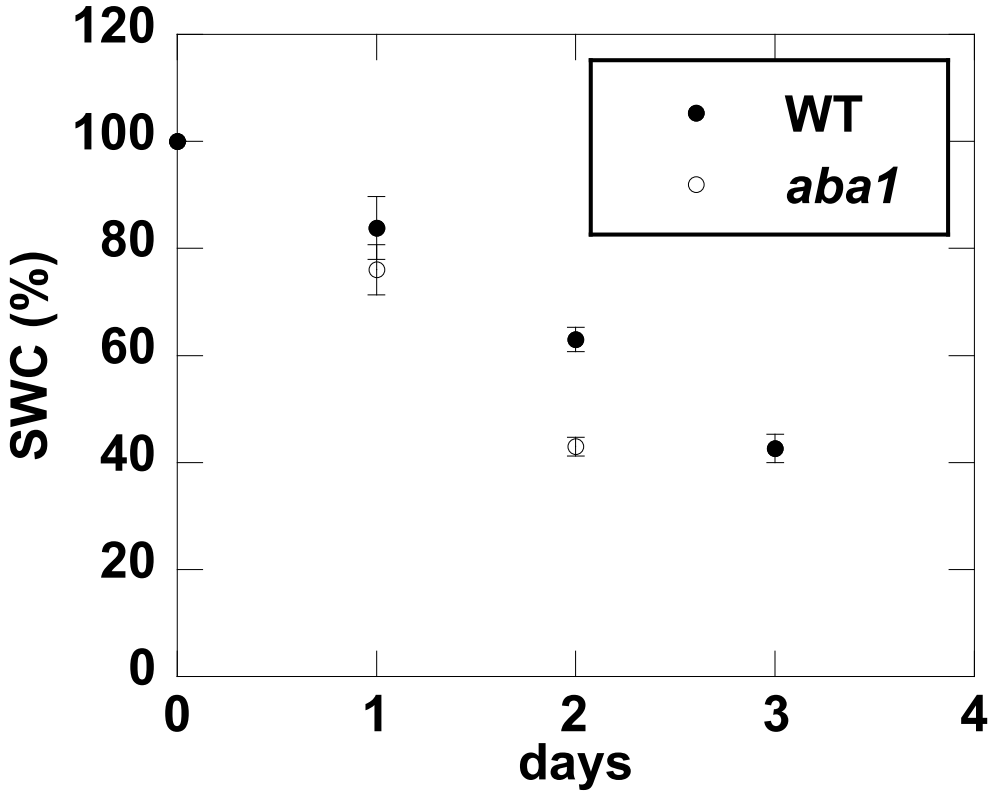

Fig.1 Changes in SWC after stopping irrigation in WT (open circles) and *aba1* (closed circles). Data are mean ± S.D, n = 4.

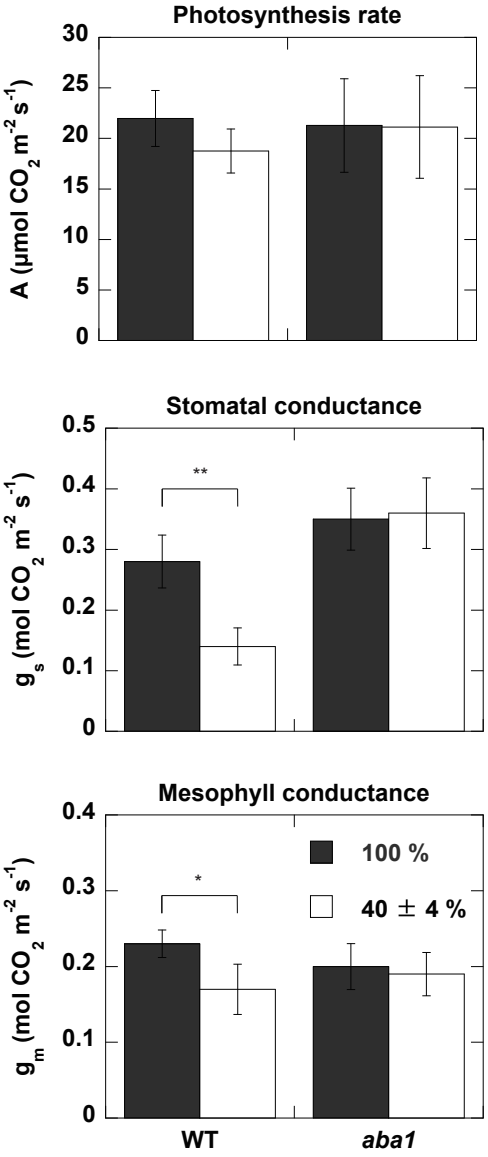

Fig. 2 Photosynthesis rate (A), stomatal conductance (g_s) and mesophyll conductance (g_m) at the SWC of 100% (solid bars) and 40±4% (blank bars) in WT (left column) and *aba1* (right column). Data are mean ± S.D. Astaliscs indicate differences between means for SWC of 100% and 40±4% (Student's *t*-test, *: P<0.05, **: P<0.01, n=5-6).

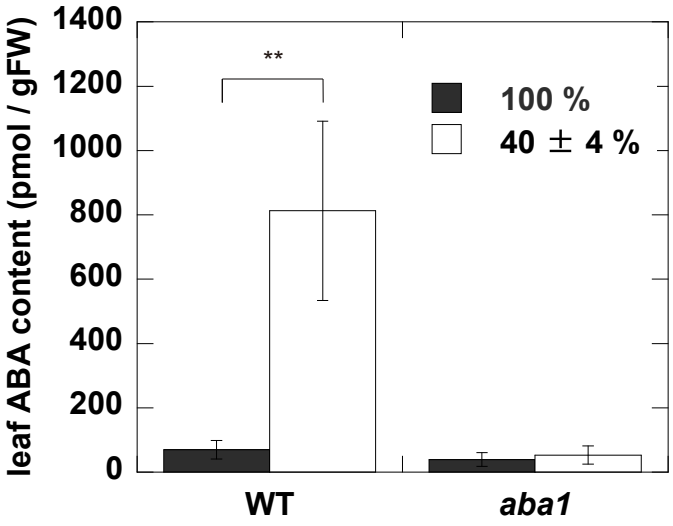

Fig. 3 Leaf ABA content at the SWC of 100% (solid bars) and 40±4% (blank bars) in WT and *aba1*. Data are mean ± S.D. Means between SWC of 100% and 40±4% were compaired by Student's *t*-test (**: $P<0.01$, n=5-6)

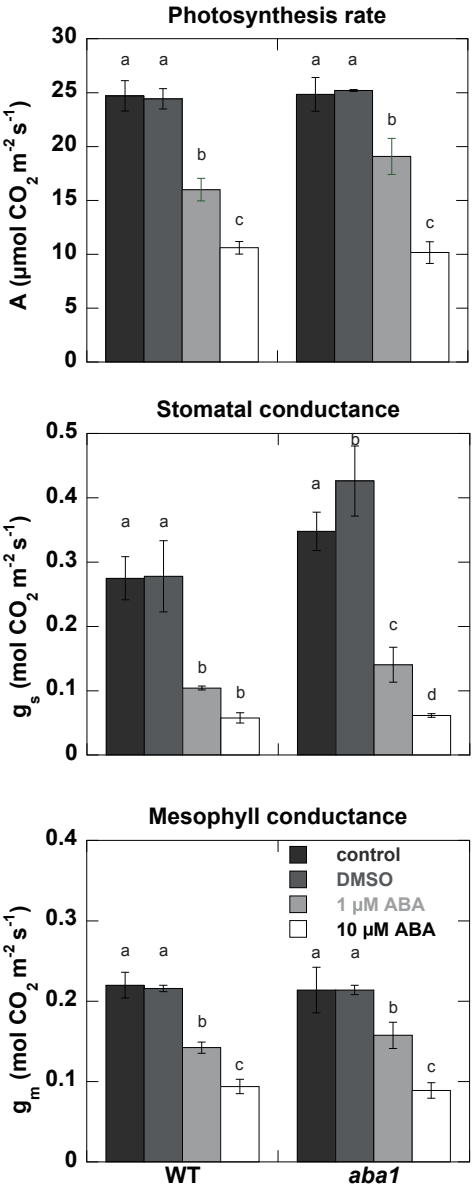

Fig. 4 Changes in A, g_s and g_m in responses to exgenously applied ABA in the artificial xylem sap. For the control, a 0.1% DMSO solution was used. Results are means ± S.D. of 3 replicates, except for the control (9 replicates). Different letters indicate significant difference between treatments at $P<0.05$ with aTukey HSD test.

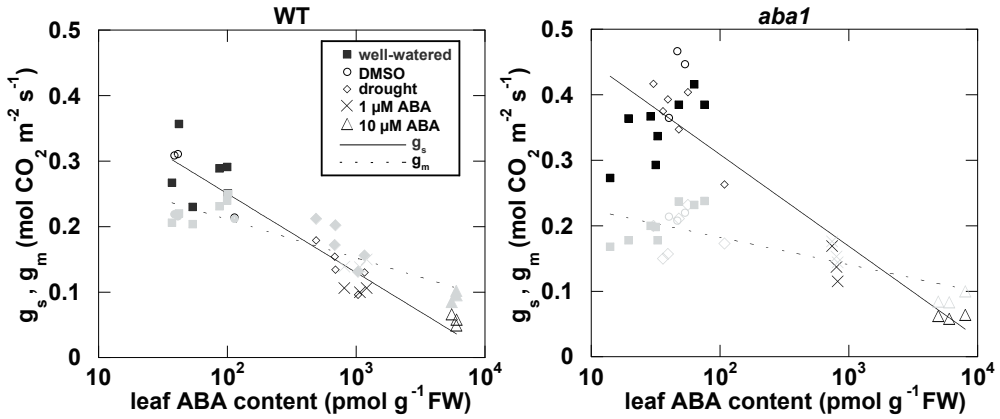

Fig. 5 The relationships between g_s (gray symbols), g_m (black symbols) and the leaf ABA content in WT and *aba1* (solid line in WT: R^2 = 0.90, dotted line in WT: R^2 = 0.79, solid line in *aba1*: R^2 = 0.78, dotted line in *aba1*: R^2 = 0.57). The data include those measured under SWC of 100% (well-watered) and 40±4%(drought), and those measured in the leaves fed with DMSO, 1 μM ABA or 10 μM ABA.

The slopes of the regression lines for g_s and g_m were statistically different in both WT and *aba1* (*ANCOVA, P*<0.01).

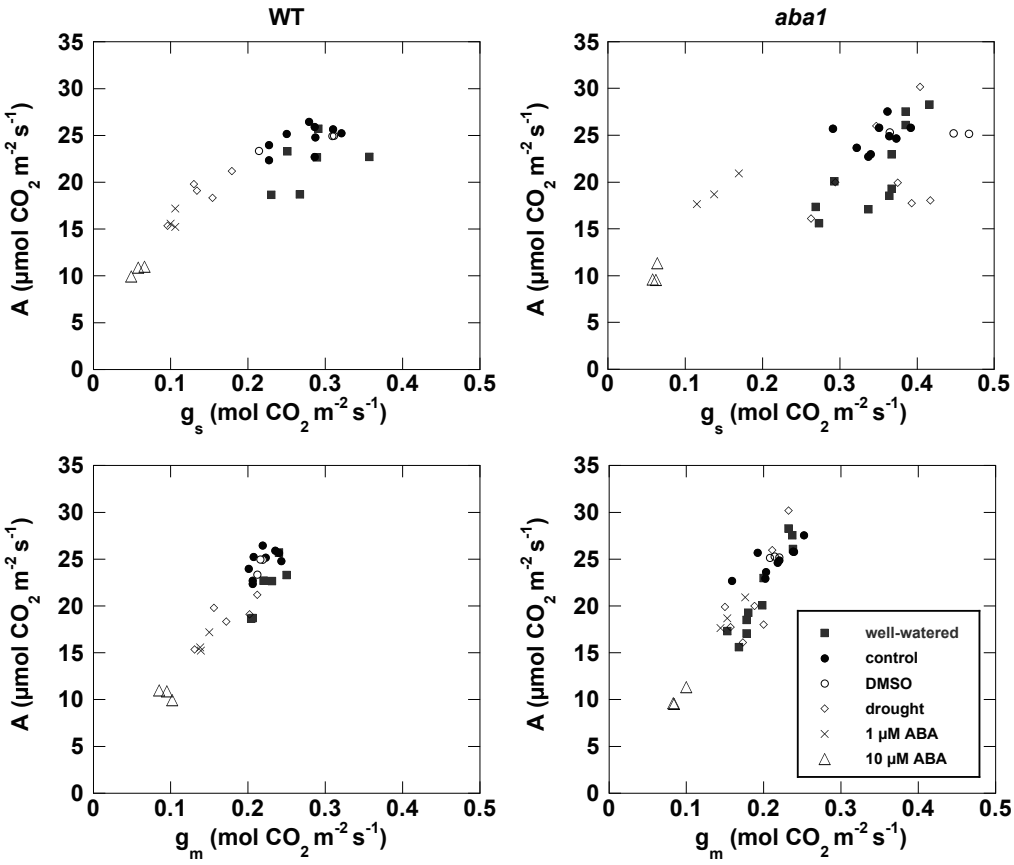

Fig. 6 The relationships between g_s, g_m and A in WT and *aba1*. The data include those measured under SWC of 100% (well-watered: filled square) and 40±4% (drought: rhombuses), and those measured in the leaves before ABA applicatio (filled circle), fed with DMSO (open circles), 1 μM ABA (x-marks) or 10 μM ABA (triangles).

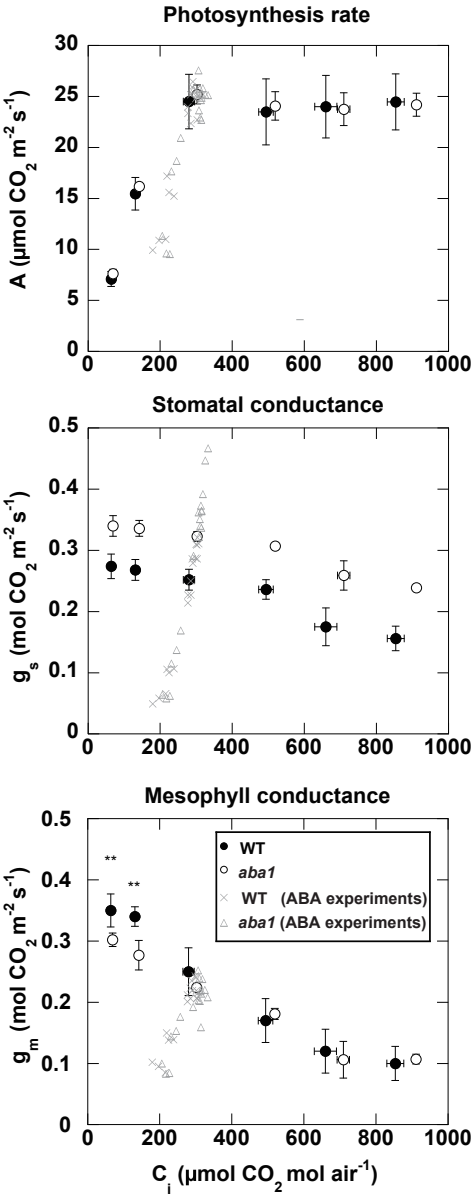

Fig. 7 CO_2 responses of A, g_s and g_m in WT (filled circles) and *aba1* (open circles). Measurements were conducted at C_a of 100, 200, 390, 600, 800 and 1000 μmol mol^{-1} at 1 % O_2. The data points are means ± S.D., n = 3. Astelisks indicate differences between means of g_m in WT and *aba1* at C_a of 100 and 200 μmol mol^{-1} (Student's *t*-test, **: $P<0.01$).

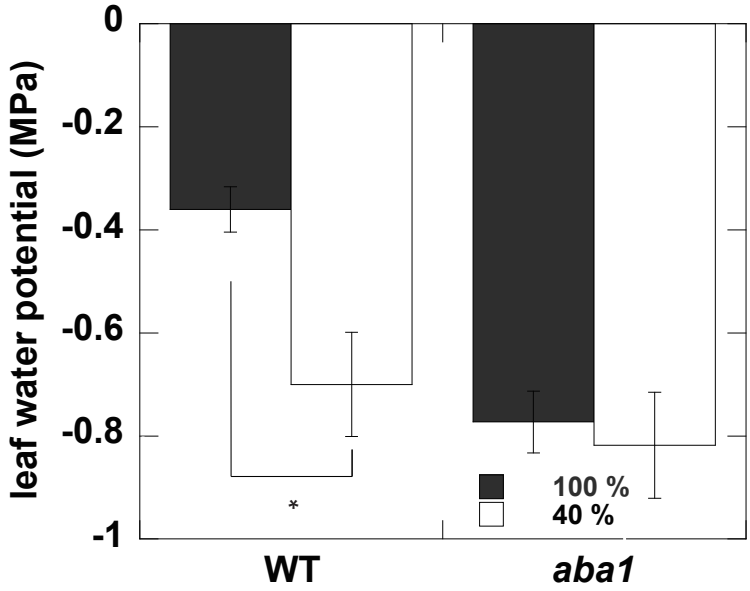

Fig. 8 Leaf water potential of the leaves at the SWC of 100% (solid bars) and 40 ± 4% (blank bars) in WT and *aba1*.

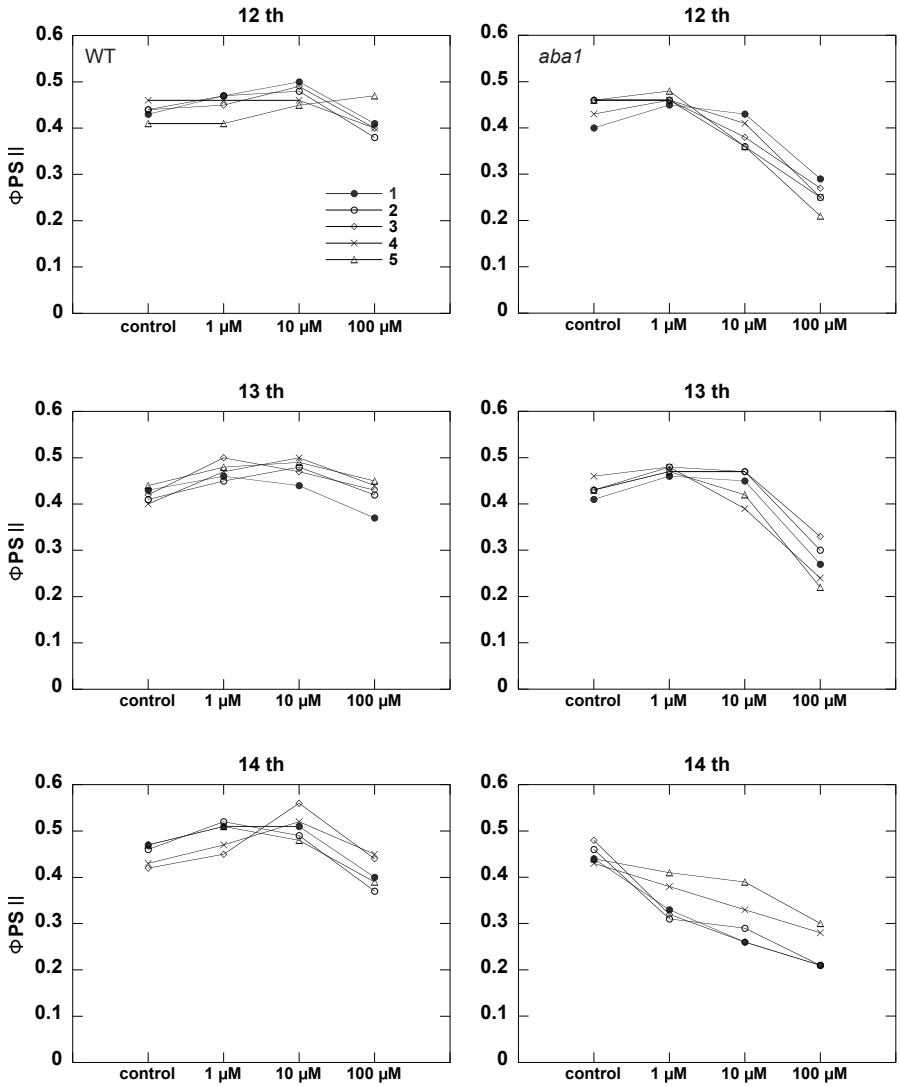

Supplementary data. 1 Leaves were progressively fed with 0, 1, 10 and 100 μM ABA solutions over about five hours. For each leaf sample, five measuring areas (each 0.02 cm^2) were randomly chosen over the leaf area of 6 cm^2 and Φ_{PSII} values at these points are compared. Different symbols denote the measuring areas.

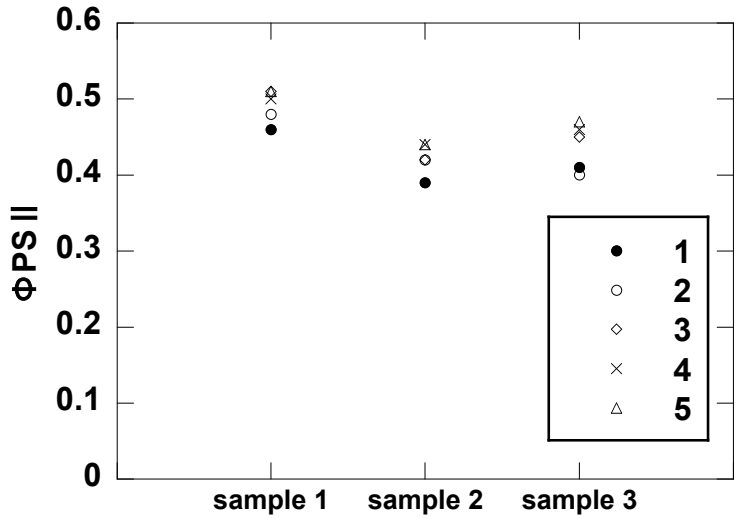

Supplementary data. 2 Φ_{PSII} were measured with three WT leaves under drought conditions at SWC of about 40 ± 4%. Different symbols denote the measuring points chosen randomly.

CHAPTER 3

Responses of CO_2 diffusion conductances to short-term and long-term elevated CO_2 in *Arabidopsis thaliana*

Introduction

Rubisco fixes CO_2 in the chloroplast storoma. Therefore, the CO_2 concentration in the chloroplast storoma (C_c) is crucial for determining the rate of photosynthesis. Inversely, C_c is determined by the photosynthetic capacity and two CO_2 diffusion conductances, *i.e.* stomatal conductance (g_s) and mesophyll conductance (g_m). These conductances vary in response to environmental changes, and many studies have reported that these conductances were co-regulated (Flexas *et al.*, 2008). Of the responses of these conductances to elevated CO_2, the decrease in g_s has been well analyzed and the underlying mechanisms have been elucidated (Negi *et al.*, 2008, Xue *et al.*, 2011). However, only a few reports have been published for CO_2 responses of g_m. It is also important to study the responses of g_m to CO_2, in addition to g_s, because g_m limits photosynthesis to a similar extent as g_s.

g_s and g_m similarly decreased with the increase in the atmospheric CO_2 in *Arabidopsis thaliana* (Flexas *et al.*, 2007a). Rapid decreases in g_s and g_m with the increase in CO_2 were also reported for tobacco (Flexas *et al.*, 2007a, Tazoe *et al.*, 2011). On the other hand, in wheat, g_m hardly decreased in response to increase in CO_2, while g_s decreased (Tazoe *et al.*, 2009). These contrasting responses to CO_2 might be due to differences in species or the methodological and/or theoretical errors.

In most of studies dealing with conductances, the model of Farquhar (Farquhar *et al.*, 1980), which does not take the re-fixation of the (photo)respired CO_2 by Rubisco into account, has been extensively used. Tholen *et al.* (2012), and Gu and Sun (2014) pointed out that the diffusion pathways of respired and photorespired CO_2 have to be

taken into account, because considerable CO_2 thus produced diffuses from mitochondria through the cytosol and chloroplast envelope to stroma and is re-fixed by Rubisco. In high CO_2, the increase in C_i and suppression of photorespiration should affect the proportion of the CO_2 that diffuses from the intercellular space to Rubisco, to that diffused from mitochondria. There are few studies estimating g_m with the improved method that takes account of CO_2 re-fixation. Moreover, these were theoretical, modeling studies. Therefore, analyses using the actually measured data are needed for a proper assessment of the effects of high CO_2 on g_m.

Short-term elevated CO_2 treatments commonly decrease g_s and g_m, except for wheat. The decrease in g_s is argued to be adaptive because it suppresses water loss. However, the meaning of the decrease in g_m is obscure. It is possible that the lowered g_m would be a transient, recoverable phenomenon. It is also possible that the lowered g_s might affect g_m, though the underlying mechanisms are not clear. To test these hypotheses, I grew *Arabidopsis thaliana* (Col-0), *open stomata 1* (*ost1*) and *slow-type anion channel 1-2* (*slac1-2*) at 390 ppm and 780 ppm CO_2 for more than 5 weeks and measured g_m at these two C_a levels. g_s in *ost1* and *slac1-2* have been characterized and their g_s are insensitive to the increase in CO_2 (Mustilli, 2002, Negi *et al.*, 2008). OST1 is a kinase and activates SLAC1 channels via phosphorylation. SLAC1 is an anion channel that has permeabilities to Cl^- and NO_3^-. High CO_2 increases HCO_3^- concentration in guard cells, and SLAC1 is activated by OST1 (Xue *et al.*, 2011). Therefore, they would be suitable materials for understanding the response of g_m to CO_2 without the effects of g_s. As long-term growth in elevated CO_2 is known to affect leaf

strucure, I investigated leaf structural traits and discussed possible effects of these traits on g_m.

Materials and methods

Plant materials and growth condition

The wild type of *Arabidopsis thaliana* (Col-0), *ost1* (a T-DNA insertion line of *OPEN STOMATA 1, OST1*: SALK_008068) and *slac1-2* (a point mutation of *SLOW ANION CHANNNEL-ASSOCIATED1, SLAC1*: point mutation at nucleotide 656) were grown in 200 mL plastic pots (TERAOKA, Osaka, Japan), each containing 1 kg of river sand (SOSEKI, Tochigi, Japan). These plants in the pots placed on trays were grown in a growth chamber with an 8 h photoperiod, at day/night temperatures of 23/21℃ and at relative humidity of 60%. Light was provided by fluorescent lamps at a photosynthetically active photon flux density (PFD) of 200 μmol photons m^{-2} s^{-1} at the leaf level. Plants were irrigated with deionized water from the tray for the first two weeks and irrigated two to three times a week to the field capacity with the Hogland solution containing 0.67 mM KNO_3, 0.67 mM $Ca(NO_3)_2$, 0.13 mM KCl, 0.13 mM $CaCl_2$, 0.3 mM $MgSO_4$, 0.27 mM NaH_2PO_4, 0.01 mM EDTAFe, 2 μM $MnSO_4$, 0.2 μM $ZnSO_4$, 0.2 μM $CuSO_4$, 0.01 mM H_3BO_3, 0.01 μM Na_2MoO_4, 0.02 mM NaCl and 0.04 μM $CoSO_4$. The total NO_3^- concentration was 2 mM. In high N experiments, the total NO_3^- concentration was 4 mM. In long-term elevated CO_2 experiments, the plants were grown in the growth chambers, CO_2 concentrations in which were controlled at 390 ppm and 780 ppm,

respectively. Here, I express the plants grown at 390 ppm chamber as 390-plants, 390-Col-0 etc. and at 780 ppm chamber as 780-plants, 780-Col-0 etc.

Gas exchange and isotopic measurements

Gas exchange measurements were performed with a laboratory-made chamber (50×55×20 mm) for *A. thaliana* as described in Tholen *et al.* (2008). To conduct measurements at 1 or 21 % O_2 conditions, the gas used in this study was made with mass flow controllers (MM-3102L-NN; LINTEC, Tokyo, Japan) with gases from N_2, O_2 and 1 % CO_2 cylinders. O_2 concentration of the gas was checked with an oxygen sensor (3080-O_2; Walz, Effeltrich, Germany). Light was provided by a metal halide lamp (PCS-UMX250; NPI, Tokyo, Japan). The PFD at the leaf level was adjusted at 600 μmol photons m^{-2} s^{-1} and monitored with a GaAs photodiode (G1738; Hamamatsu Photonics, Hamamatsu, Japan) placed in the chamber during the measurements. The GaAs sensor was calibrated against a quantum sensor (LI-190SA and LI-1000, LI-COR, Lincoln, NE, USA). The leaf temperature and vapor pressure deficit (VPD) were kept at 22 ℃ and 0.65 ± 0.1 kPa. Isotope measurements of air entering and leaving the chamber were made as described in CHAPTER 2.

Short-term responses of g_m to the elevated CO_2 were examined as follows. At first the chamber CO_2 concentration was kept at 390 ppm and when the leaf photosynthesis attained its steady-state, the gas exchange and isotope measurements were made. After the measurements at 390 ppm, CO_2 concentration in the chamber was switched to 780 ppm and the measurements were made every 30 min up to 2 h.

For 390-plants, the measurements were started at 390 ppm and then the CO_2 concentration was switched to 780 ppm. For 780-plants, the measurements were started at 780 ppm and then the CO_2 concentration was switched to 390 ppm.

CO_2 response curves were made after these measurements. The CO_2 concentration in the chamber was changed as follows in a stepwise manner from 200, 100, 50, 390, 600, 780 to 1000 ppm for both 390- and 780- plants. The dark respiration rate was measured after these measurements at 390 ppm and 780 ppm. These measurements described above were conducted at 1% O_2. All these measurements using the 390- and 780-plants were repeated at the O_2 concentration of 21%.

Calculation of mesophyll conductance and sensitivity analyses of g_m to b, R_d and Γ*

Calculation of the mesophyll conductance was conducted in almost the same way as described in CHAPTER 2, but some of the parameters were different. Mesophyll conductance was calculated as

$$g_m = \frac{\left(b - a_i - \frac{eR_d}{A + R_d}\right)\frac{A}{C_a}}{a_b + (a_s - a_b)\frac{C_{as}}{C_a} + (b - a_s)\frac{C_i}{C_a} - \frac{eR_d(C_i - \Gamma^*)}{C_a(A + R_d)} - \frac{f\Gamma^*}{C_a} - \Delta}$$

where C_a is the ambient CO_2 concentration, C_{as} is the CO_2 at the leaf surface, C_i is the intercellular CO_2, C_c is the CO_2 at the chloroplast stroma, a_b and a_s are the carbon isotope discriminations caused by diffusion through boundary layer (2.9‰) and stomata

(4.4‰), respectively, a_i is the carbon isotope discrimination during CO_2 diffusion/hydration through water (1.8‰), and b is the carbon isotope discrimination caused by the carboxylation reaction by Rubisco and phospho*enol*pyruvate carboxylase (30‰). e was calculated as follows as described in CHAPTER 2

$$e=\delta^{13}C_{\text{gas cylinder}} - \delta^{13}C_{\text{atmosphere}}.$$

In the experiments described in this chapter, $\delta^{13}C_{\text{gas cylinder}}$ was – 34.36‰ and the carbon isotope composition in the 390 ppm and 780 ppm growth chambers, $\delta^{13}C_{\text{atmosphere}}$, were assumed to – 9.94‰ and –16.88‰, respectively, the average values of five replicates. Therefore, e was set to – 24.42‰ and –17.48‰. The day respiration rate (R_d) is assumed to be the same as the dark respiration rate (R_{dark}). The symbols f (11.6‰) and Γ^* are the carbon isotope discrimination during photorespiration and a CO_2 compensation point without the day respiration, respectively (Lanigan *et al.*, 2008). Γ^* was measured using the Laisk method with 390- and 780-Col-0, respectively (Laisk, 1977).

To calculate g_m with the method used in Gu and Sun (2014), I used the simplified equation as follows:

$$g_m = \frac{(1+t)A(b-a_i-\frac{\beta_b}{\beta_e}e\frac{R_d}{(A+R_d)})}{a_bC_a+(a_s-a_b)C_{as}+(1+t)\left(\frac{\beta_b}{\beta_e}e\frac{R_d}{A+R_d}-\frac{\beta_b}{\beta_e}f\right)\Gamma^*+(1+t)\left(b-a_s-\frac{\beta_b}{\beta_e}e\frac{R_d}{A+R_d}\right)C_i-(1-t)C_a\Delta^{13}}$$

β_b and β_e denote 1+b and 1+e, respectively. t is the ternary effect factor and equals to $\frac{(1+\bar{a})E}{2g_t}$, where g_t is the total conductance to CO_2 including boundary layer and stomata. $\bar{a}$ is the weighted fractionation as follows:

$$\bar{a} = \frac{a_b(C_a - C_{as}) + a_s(C_{as} - C_i)}{C_a - C_i}.$$

Consideration of ternary effect for the plant isotopic model was first proposed by Farquhar and Cernusak (2012), and this effect is due to the influence of the transpiration mass flow to CO_2 discrimination across the leaf boundary layer and stomata.

Sensitivity analyses were conducted with the data obtained for the CO_2 response curves with Col-0. The g_m to C_i response curves were analyzed with changing Rubisco fractionation factor b from 27 to 32‰, R_d from –0.5 to –1.5 μmol CO_2 m^{-2} s^{-1} and Γ* from 5 to 15 μmol CO_2 mol air^{-1} for 1% O_2 measurements and 35 to 45 μmol CO_2 mol air^{-1} for 21% O_2 measurements.

$\delta^{13}C$ and Δ of leaf dry matter

Fully expanded leaves were collected and dried at 80℃ for more than two days. Dried leaf samples were crushed using beads and Multi-Beads Shocker (MB501U; YASUI KIKAI, Osaka, Japan). Leaf samples,1.5 mg each, were used for isotope analysis. Carbon Isotope analysis was conducted with a stable isotope spectrometer

(Isoprime; Isoprime Ltd, Manchester, UK) combined with an elemental analyzer (Vario Micro; Elementar, Hanau, Germany). Carbon isotope ratio was expressed as $\delta^{13}C$ calculated as

$$\delta^{13}C = \frac{R_{sample}}{R_{standard}} - 1$$

where R_{sample} and $R_{standard}$ are the carbon isotope ratios of the leaf dry sample and the standard, PeeDee belemnite, respectively.

Δ was calculated as

$$\Delta = \frac{\delta_a - \delta_p}{1 + \delta_p}$$

where δ_a was the carbon isotope ratio of the air in the growth chamber and δ_p was the carbon isotope ratio of the leaf dry sample.

S_c and structural traits

Leaf segments were cut off with a razor blade and immediately immersed in the 80 mM Sørensen's phosphate buffer (pH7.2) containing 3% formaldehyde and 4% glutaraldehyde and vacuum-infiltrated. The segments were washed with the phosphate buffer and then dehydrated with ethanol series. The segments were embedded in Technovit 7100 (Heraeus Kulzer, Hanau, Germany). Transverse and paradermal

sections at 1 μm thick were cut on a ultramicrotome (Reichert Ultracut S, Leica, Vienna, Austria) and stained with 1% toluidine blue-O and photographed with a digital camera (DP71; Olympus, Tokyo, Japan) under a light microscope (BX50; Olympus) at magnification of 200-fold. The images were analyzed with Image-J, Ver 10.2.

The surface area of mesophyll cell walls exposed to intercellular air space (S_{mes}) and surface area of chloroplasts facing the intercellular air space (S_c) were calculated as

$$S_{mes} = \frac{L_{mes}}{w} F$$

$$S_c = \frac{L_c}{w} F$$

where L_{mes} is perimeter length of mesophyll cells exposed to intercellular air space obtained from transverse sections, L_c is length of chloroplasts facing the intercellular air space obtained from transverse sections, w is the width of the image used for measurements with transverse sections, F is the curvature correction factor suggested in Thain (1983). To determine F, I measured the width of palisade cells and spongy cells using the paradermal sections, and heights of palisade tissue cells and spongy tissue using the transverse sections.

A commercially available adhesive (Cemedine; Cemedine, Tokyo, Japan) was applied to the abaxial surfaces of fully expanded leaves. When the adhesive was completely dried, it was peeled and 5 images were photographed for one leaf under the light microscope at 200-fold magnification.

Results

Short-term responses to elevated CO_2

In the short-term elevated CO_2 experiment, photosynthesis rate did not change while g_s and g_m were decreased in Col-0. C_c in Col-0, *ost1* and *slac1-2* was changed from 213.9 to 500.0, 229.6 to 555.3 and 215.5 to 556.6 μmol CO_2 mol air^{-1}, respectively, when CO_2 concentration around the leaf was switched from 390 ppm to 780 ppm (Fig. 1). Because these measurements were conducted at 1% O_2 concentration and in relatively high light (600 μmol photon m^{-2} s^{-1}), C_c would be high enough to maximize A even at 390 ppm. Judging from the A-C_i relationships shown in Fig. 3, this would be the case. Apparently g_s in *ost1* and *slac1-2* did not respond to the elevated CO_2 (Fig. 1) as the previous studies had already reported (Negi *et al.*, 2008, Tazoe *et al.*, 2011, Xue *et al.*, 2011). g_m in *ost1* and *slac1-2* decreased in the elevated CO_2 in the same manner as that in Col-0. g_s and g_m decreased in 30 min after the switching of CO_2 concentration (Fig. 1).

Responses of photosynthetic characteristics to long-term elevated CO_2

In the long-term elevated CO_2 experiments with low N plants, the plants grown at 390 ppm CO_2 (390-plants) showed somewhat higher photosynthesis rates than 780-plants when the rate of photosynthesis was measured at the PFD of 600 μmol photons m^{-2} $s^{-1}$and 390 ppm CO_2 although the differences were not statistically significant (Fig. 2). After the long-term growth at 390 or 780 ppm CO_2 at 2 mM N, the photosynthesis rates measured at the PFD at 600 μmol m^{-2} s^{-1} at 390 ppm CO_2 in the

plants grown at 390 ppm (390-plants) were comparable to those in 780-plants (Fig. 2). The photosynthetic rates at 780 ppm were also comparable (Figs. 2, 3).

As shown in Fig. 2, g_s was higher in *ost1* and *slac1-2* than in Col-0 regardless of the growth and measurement conditions. g_s in *slac1-2* hardly changed in all the measurements and growth conditions, while g_s in 390-*ost1* was higher than 780-*ost1* when the measurements were made at 780 ppm. g_s in *ost1* was insensitive to the elevated CO_2 but their abilities to respond to light and low CO_2 were kept normal. Because it was very dark when I picked up the sample in the growth chamber, therefore, g_s in *ost1* would be low. The photosynthetic characteristics of the 780-*ost1* were measured at 780 ppm at first. Thus, the conditions would not induce opening of stomata. On the other hand, the measurement with 390-*ost1* was started at CO_2 concentration of 390 ppm, therefore, it would induce opening of their stomata.

g_m in all genotypes were lower when measured at 780 ppm than at 390 ppm regardless of the growth conditions. These results implied that, in the plants grown at 780 ppm, g_m levels were kept low during the long-term growth.

CO_2 response curves

When A-C_i curves were obtained at 1% O_2, initial slopes of 780-plants were lower than 390-plants in all genotypes (Fig. 3). However, there were no differences in initial slopes between 390- and 780-plants when A-C_i curves were obtained at 21% O_2 (Fig. 4). In the high C_i region, A slightly decreased with the increase in C_i at 1% O_2 probably because limitation in the triose phosphate utilization (Sharkey *et al.*, 2007).

g_s decreased with the increase in C_i in Col-0 at both 1% and 21%. However, as Fig. 1 also demonstrated, g_s kept at high levels irrespective of increasing in C_i in both *ost1* and *slac1-2* at both 1% and 21% O_2. As already mentioned above, there were some low values of g_s in *ost1* because these plants retained ability to decrease g_s in response to low light, and that situation might occur when I moved plants from the growth chamber to the measurement system. In addition, 780-plants were at first subject to the measurements at 780 ppm, the condition which did not induce quick increases in g_s.

g_m decreased with the increase in C_i and there were not significant differences in the response between 390- and 780-plants at both 1% and 21%. However, the responses of g_m to C_i were somewhat smaller at 21% O_2 compared with 1% O_2 (Figs. 3, 4).

Sensitivity analyses of g_m to b, Γ* and R_d

Because Γ* is one of the important parameters determining g_m, Γ* (C_i*) was measured with Laisk method. Γ* (C_i*) responded to O_2 concentration as reported in Laing *et al.* (1974), and Γ* (C_i*) differed by about 7 μmol CO_2 mol air^{-1} between two CO_2 growth conditions at 20% O_2 (Fig. 5). Y-intercepts also differed. As pointed out by previous studies, Γ* measured with Laisk method is not the true Γ*, and often expressed as C_i* because g_m was ignored in the Laisk method (Gu & Sun, 2014). Therefore, sensitivity analyses were needed for accurate investigation of g_m responses to C_i. Other important parameters were b and R_d because b is the significant fractionation factor that

might have a large effect on calculation of g_m as suggested by Tazoe *et al.* (2011), and Gu and Sun (2014), and R_d were often measured with Laisk method, though R_d was considered as the same value as dark respiration rate in this study. I used Col-0 data for the sensitivity analyses. Rubisco fractionation factor b had the largest effect on g_m calculation (Fig. 6). Original value of b used in this study was 30‰. Because 27 to 32‰ were used for other studies, I calculated with these b values. The sensitivity of g_m measured at 21% O_2 to the fractionation factor b was lager than g_m measured at 1% O_2. For sensitivity analyses of R_d, variation of R_d had a smaller effect on calculation of g_m than b. However, again, the data measured at 21% O_2 were more sensitive to variation of R_d. Γ* exerted the smallest effect on calculation of g_m.

According to Gu and Sun (2014), calculation of g_m should be improved by including estimation of the re-fixation of CO_2 from mitochondria. Therefore, I used their equations to estimate g_m and conducted sensitivity analyses. In the data analyses with their method, responses of g_m to C_i were less at 21% O_2 than at 1% O_2, but g_m was still sensitive to C_i (Fig. 7). The fractionation factor b had the largest effect on calculation of g_m, however, the effects were smaller than the analyses with the conventional equations for calculating g_m.

Photosynthetic characteristics with high N grown plants

Evans *et al.* (1994) demonstrated that Rubisco content related to g_m (CO_2 transfer conductance). Therefore, I grew plants at the doubled NO_3^- of 4 mM, and measured photosynthetic characteristics.

780-plants showed greater A than 390-plants at measuring CO_2 of 780 ppm in all genotypes (Fig. 2). Unfortunately, the data of *slac1-2* were obtained with another batch of plants that were one week older than the others, because of a machine trouble.

Almost the same results as the experiment with the lower N plants were obtained for g_s. 780-plants grown with higher N had larger g_m than those grown at lower N at the both measurement CO_2 conditions. In addition, in case of higher N experiments, 780-Col-0 and 780-*ost1* had slightly larger g_m than 390-Col-0 and *ost1* plants measured at 780 ppm CO_2.

Structural traits, **leaf $\delta^{13}C$ and composition of leaves**

Leaf thickness was not affected by growth CO_2 level irrespective of the N nutrition level. On the other hand, the NO_3^- level affected leaf thickness and the leaves of 4 mM plants were thicker than those of 2 mM plants N (Table. 1). S_m and S_c were unchanged under all growth conditions. 780-Col-0 had greater LMA than 390-Col-0, and 4 mM N leaves showed greater LMA.

In 390-plants irrespective of the growth N conditions, *ost1* and *slac1-2* had slightly smaller $\delta^{13}C$ than Col-0 probably because they had greater g_s than Col-0 (Fig. 8). The differences became larger in 780-plants. This was probably due to the fact that Col-0 closed their stomata in response to high CO_2 while stomata in *ost1* and *slac1-2* were insensitive to high CO_2, as shown in short term responses of g_s. These data supported that stomata in *ost1* and *slac1-2* were kept insensitive to high CO_2 during their growth period.

The N content of leaf dry matter depended on growth CO_2 concentration and NO_3^- concentration. Higher CO_2 growth condition and lower NO_3^- concentration decreased N (Fig. 9). Cultivation at 780 ppm slightly increased C in high N plants but not in low N plants. Therefore, changes in C/N ratio in the leaf largely depended on changes in N of the leaf.

Stomatal densities of *ost1* (390 ppm) and *slac1-2* (390 ppm) were slightly higher than Col-0 (Fig. 10). Higher CO_2 growth condition decreased the stomatal density only in *ost1*.

Discussion

It has been reported that g_s and g_m decrease simultaneously at elevated CO_2 condition (Flexas *et al.*, 2012, Flexas *et al.*, 2007a, Tazoe *et al.*, 2011, Vrabl *et al.*, 2009). The responses of g_s to changing in CO_2 concentration around leaves have been well analyzed and the mechanisms have been elucidated (Negi *et al.*, 2008, Xue *et al.*, 2011). In contrast, the responses of g_m to elevated CO_2 were poorly understood. Or, even the fundamental question, whether or not g_m changes with CO_2 concentration, is still controversial, because the responses differ markedly depending on the plant species and methods to estimate g_m (Flexas *et al.*, 2008, Gu & Sun, 2014, Tazoe *et al.*, 2009). Therefore, I carefully consider the method to estimate g_m and parameters for the calculation of g_m. Further, elevated CO_2 is known to induce stomatal closure in both short-term and long-term. Therefore, I used two mutants of *Arabidopsis thaliana*

stomata of which are insensitive to elevation of CO_2, to avoid possible influence of stomatal closure on g_m estimation.

According to the present analyses of photosynthetic characteristics, responses of g_s and g_m to the elevated CO_2 were independent in both short-term and long-term experiments (Fig. 1-4). It has been shown that the simultaneous decreases in g_s and g_m occur in response to drought condition, salinity and elevated CO_2 (Flexas *et al.*, 2008). However, there have been few studies demonstrating independent responses of g_s and g_m to environmental changes. One of such studies is Tazoe *et al.* (2011), and they first reported the independent responses of g_s and g_m to elevated CO_2 using *ost1* mutant (Landsberg *erecta* back ground). There are some differences between their results and the present results. In Tazoe *et al.* (2011) the differences were not significant and g_m in *ost1* was lower than that of WT while g_s was higher than that of WT. In the present study, the differences were not significant, but g_m in *ost1* and *slac1-2* were slightly lower than that in Col-0, while *ost1* and *slac1-2* had higher g_s than Col-0 (Fig. 2). The compensating regulation of g_m in response to g_s might be mediated by C_i, because slightly greater g_s in *ost1* and *slac1-2* caused higher C_i. However, in the plants grown at high N, there was no such tendency as mentioned above (Fig. 2).

In the long-term CO_2 experiment, g_m in the 780-plants was the same level as g_m in 390-plants when measurements were made at 780 ppm (Fig. 2). These results suggested that the decrease in g_m at elevated CO_2 was not a transient phenomenon and the plants could not have so high g_m as that in 390-plants. On the other hand, 780-Col-0 and 780-*ost1* grown at high N nutrition tended to have larger g_m than

390-Col-0 and 390-*ost1* when measurements were made at 780 ppm (Fig. 2). Further, plants grown at high N had higher g_m than that with low N nutrition (Fig. 2). It has been reported that the N content and Rubisco content in the leaves strongly correlate with g_m (Evans *et al.*, 1994, Warren, 2004). These correlations have been explained as the changes of structural traits. In high N plants, surface area exposed to intercellular air space (S_c) would increase and thereby increase g_m. However, in this study, there were no significant differences in S_c among the plants (Table. 1). The discrepancy between the present study and the previous studies may arise from several reasons. (1) Evans *et al.* (1994) have used Rubisco small subunit antisense line in tobacco, and A of this line was half of that in WT. Differences in A between plants grown with high N and low N in my study was not marked, only about 5 μmol CO_2 m^{-2} s^{-1} at maximum, therefore, S_c might not be different (Fig. 2, Table. 1). (2) S_c was already at maximum level even in the plants grown with 2 mM N. According to Tholen *et al.* (2008), who examined effects of chloroplast movement on S_c and photosynthesis, the increase in S_c resulted in higher A and g_m. In this case, S_c increased and this brought about the increase in A. When the present S_c and S_c /S_m were compared with their data, both of these values were quite high. Therefore, there might be no room for increasing S_c.

For the different responses of g_m in Col-0 and *ost1* to elevated CO_2 between the plants grown at high N and those grown at low N (Fig. 2), the carbohydrate levels might be a key factor. Elevated CO_2 affects carbon metabolisms, and increases non-structural carbohydrates including glucose, fructose, sucrose and starch (Leakey *et al.*, 2009, Sims *et al.*, 1998). The leaf mass per unit area (LMA) of plants grown at elevated CO_2

was greater than that at ambient CO_2 supported this idea (Table. 1). In addition, N level also affects this carbon metabolisms, and plants grown with high N have lower non-structural carbohydrate than that with low N (Sims *et al.*, 1998). Although Rubisco content was not measured in this study, Rubisco content per unit leaf area (g m^{-2}) could be estimated from the data of LMA and nitrogen content (%) of leaf dry matter in this study (Table.1, Fig. 9). N per leaf area of the leaves in 390- and 780-Col-0 grown at low N, and 390- and 780-Col-0 grown at high N, were 0.37, 0.58, 1.19 and 1.02 g N m^{-2}, respectively. 30～40% of these nitrogen would be assumed to be in Rubisco. Therefore, in this study, Rubisco content probably increased in plants grown at high N to a considerable extent. On the other hand, 780-plants at low N would have more non-structural carbohydrate than those grown at high N. If chloroplasts have higher level of non-structural carbohydrate, chloroplasts might become thicker because of storage of starch. Araya *et al.* (2006) and Nafziger and Koller (1976) argued that the g_m decreased with the increase in starch content. The different response of g_m to elevated CO_2 between high N and low N grown plants could be attributed to the difference in the starch content in the chloroplast, however, rapid decrease in g_m in response to elevated CO_2 may not be explained by changes in S_c or carbohydrate contents.

There are several possibilities to explain the rapid decrease in g_m in response to elevated CO_2. One is the artefact in the g_m calculation. Tholen and Zhu (2011) developed a 3D CO_2 diffusion model in the liquid phase to evaluate the influence of re-fixation of respired and photorespired CO_2, because previous CO_2 diffusion models have not evaluated re-fixation of CO_2 well. In addition, Tholen *et al.* (2012) and Gu and

Sun (2014) developed new methods to estimate g_m, which take account of estimation of CO_2 re-fixation. As shown in Fig. 7, when the data of CO_2 response curves were re-calculated with the equation of Gu and Sun (2014), all the data were somewhat less than the data calculated with the conventional equation in Tazoe *et al.* (2011). Being similar to the calculations by Tazoe *et al.* (2011), g_m measured at 21% O_2 were less sensitive to C_i. However, the decreases with C_i were still statistically significant. g_m measured at 1% O_2 was responded to C_i markedly even when g_m was estimated with (Gu & Sun, 2014). When R_d was set to -1.5 μmol CO_2 m^{-2} s^{-1} in the sensitivity analyses, responses of g_m to C_i seem to be completely diminished. However, R_d of -1.5 μmol CO_2 m^{-2} s^{-1} was not a physiologically possible value. R_{dark} was about -0.8 μmol CO_2 m^{-2} s^{-1} in this study. Therefore, it is quite unlikely to have larger R_d than R_{dark}. When sensitivity analyses were conducted with the data measured at 1% O_2, whatever b, R_d and Γ* values were, g_m decreased with the increase in C_i. All these examinations clearly show that the decrease in g_m with the increase in CO_2 is not an artifact.

Considering very rapid nature of the changes some mechanism would be proposed. One possible explanation might be the leakiness of HCO_3^- through the chloroplast envelope. According to the simulation in Tholen and Zhu (2011), if the permeability of HCO_3^- across the chloroplast envelope is more than 5×10^{-7} m s^{-1}, the decrease in g_m in response to high C_i can be explained. Because of the difference in pH and CO_2 concentration, the concentration of HCO_3^- in the chloroplast stroma is higher than that in the cytosol. When the CO_2 concentration is elevated, HCO_3^- in the chloroplast stroma leaks to cytosol, and g_m would be decreased.

Other possible biochemical factors include carbonic anhydrase (CA) and aquaporins. CAs on the plasma membrane, cytosol and chloroplast catalyze the equilibrium between HCO_3^- and CO_2. As I mentioned above, the concentration of HCO_3^- in chloroplast stroma might be a key factor to determine the leak flow, and therefore CA concentration might be important.

Plasma membrane intrinsic proteins (PIP) or aquaporins might be important. It has been reported that the amount of some PIPs regulated g_m (Flexas *et al.*, 2006b, Hanba *et al.*, 2004, Uehlein *et al.*, 2012). However, the relationship between PIPs and decrease in g_m in response to CO_2 is still ambiguous. One possible explanation for the rapid decrease in g_m is changes in the activation state of PIPs. It was reported that PIP activity was controlled by phosphorylation and protonation might be possible in roots (Prak *et al.*, 2008, Tornroth-Horsefield *et al.*, 2006). While it is not likely that the bulk amount of PIPs changes very quickly, membrane dynamics reported for H^+-ATPase in stomatal guard cells (Hashimoto-Sugimoto *et al.*, 2013) could be possible. Clearly further studies are needed.

In this chapter I conducted detailed analyses of g_m in response to CO_2 under various conditions, and revealed and/or confirmed several features. i) The decrease in g_m in response to elevated CO_2 occurred independent of the changes in g_s. Analyses with mutants showed that g_m decreased independently from the behavior of g_s. ii) The extent of the decrease in g_m depended on O_2 concentration. The greater decrease in g_m was observed at 1% O_2 than at 21% O_2. iii) Nitrogen nutrition and CO_2 levels during the growth affected responses of g_m to elevated CO_2. The difference might be due to

changes in chloroplast starch metabolism. With the decrease in CO_2 concentration and/or nutritional N level, starch tended to accumulate, which would decrease g_m without changes in S_c.

Recently, the decrease in g_m with the CO_2 level has been challenged as the artifact in the conventional method. I carefully took account of suggestions byTholen and Zhu (2011), Tholen *et al.* (2012) and Gu and Sun (2014) and improved the equations for estimating g_m. Therefore, the present results would be a framework to re-evaluate g_m response to CO_2.

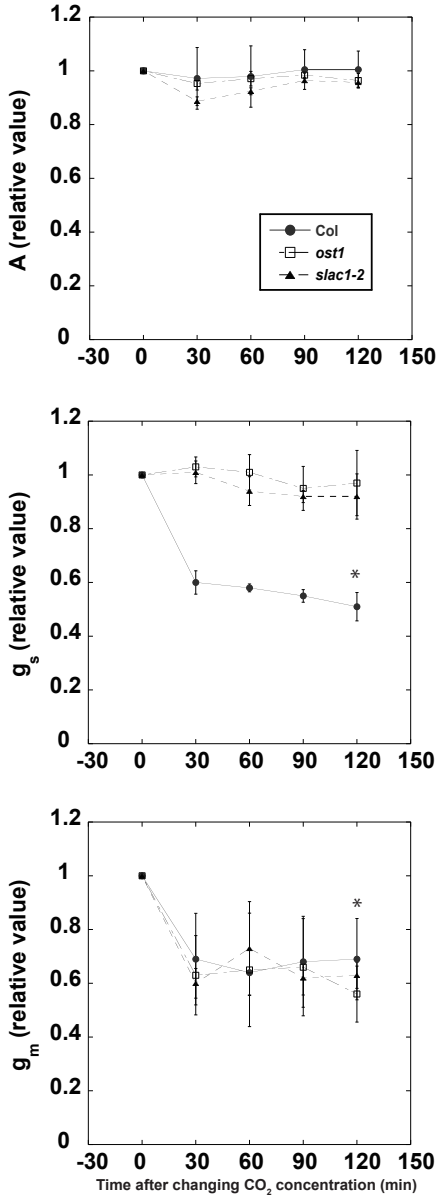

Fig. 1 Short-term responses of photosynthetic characteristics to elevated CO_2 at 1% O_2. 0 min means the time when CO_2 concentration around the leaves switched from 390 ppm to 780 ppm. Data are mean ± S.D. (n=3-5). * indicates difference between the means at 120 min and 0 min (Student's *t*-test, $P<0.05$).

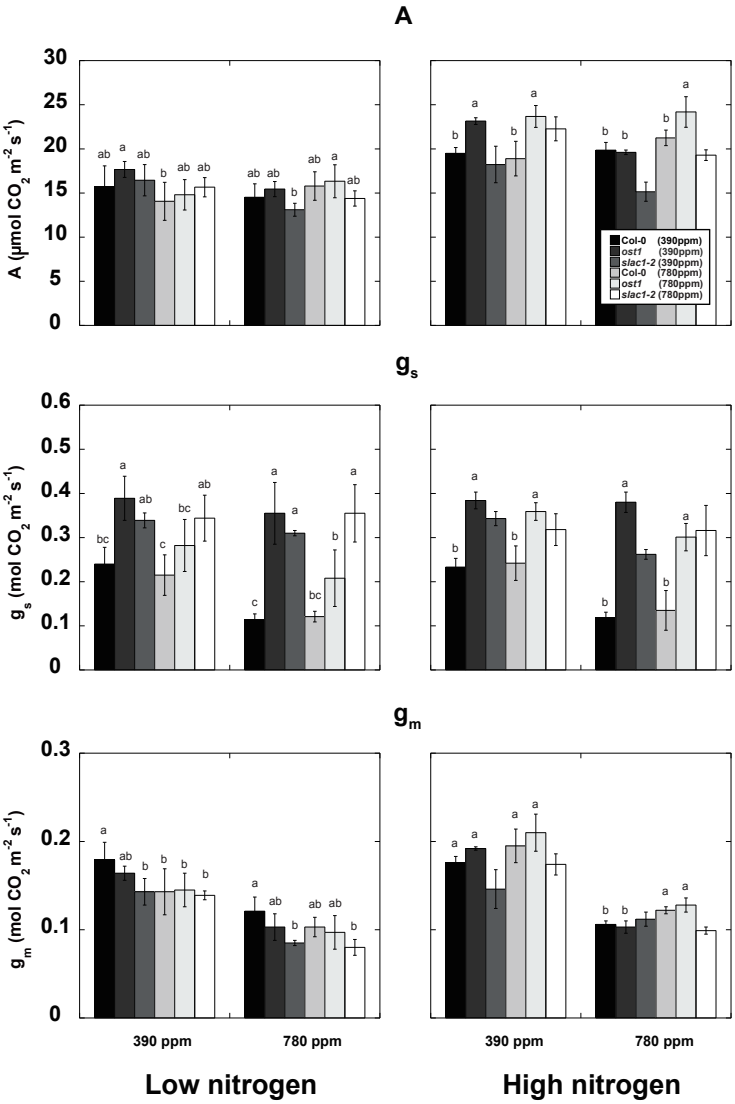

Fig. 2 Photosynthetic characteristics of the plants grown at 390 ppm and 780 ppm at low and high nitrogen nutrition levels. Left columns indicate the data measured at 390 ppm and right side ones measured at 780 ppm. Darker three columns (left three columns of left six) are plants grown at 390 ppm. Whiter three represent plants grown at 780 ppm. Data are mean ± S.D. (n=3-6). Different letters indicate significant differences analyzed with Tukey's HSD for six (low nitrogen) or four (high nitrogen) columns as one batch ($P < 0.05$). The data in *slac1-2* (390, 780 ppm) with high nitrogen were excluded for Tukey's HSD because they were measured with another batch of the plants as mentioned in the text.

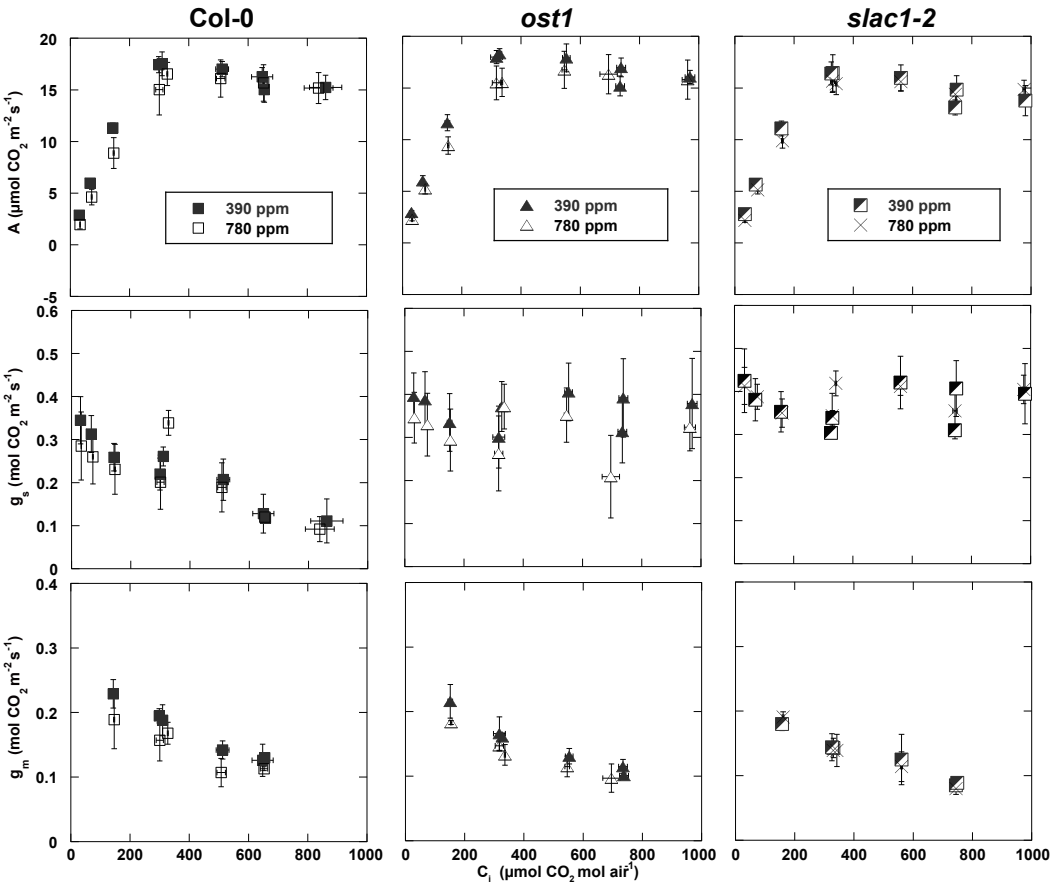

Fig. 3 CO_2 responses of the photosynthetic characteristics measured at 1% O_2. Filled marks are plants grown at 390 ppm and others are plants grown at 780 ppm. Data are mean ± S.D. (n=3-4).

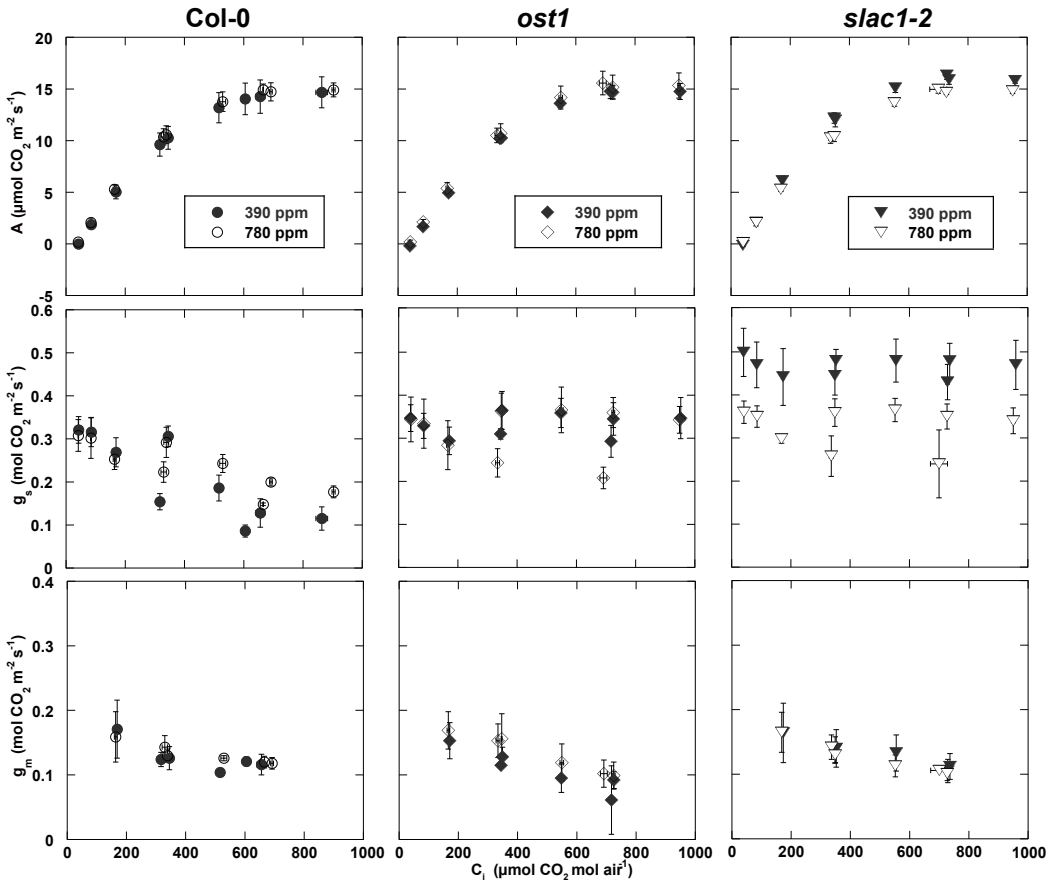

Fig. 4 CO_2 responses of the photosynthetic characteristics measured at 21% O_2. Filled marks are plants grown at 390 ppm and others are plants grwon at 780 ppm. Data are mean ± S.D. (n=3).

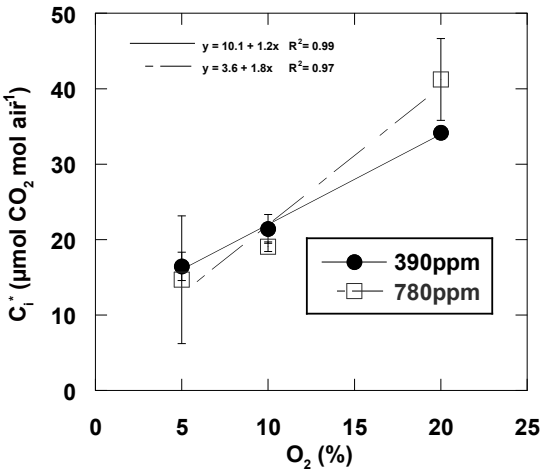

Fig. 5 Relationships between Γ* (C_i*) and O_2 concentration in Col-0 grown at 390 ppm (filled circles) or 780 ppm (blank square). Data are mean ± S.D. (n=3).

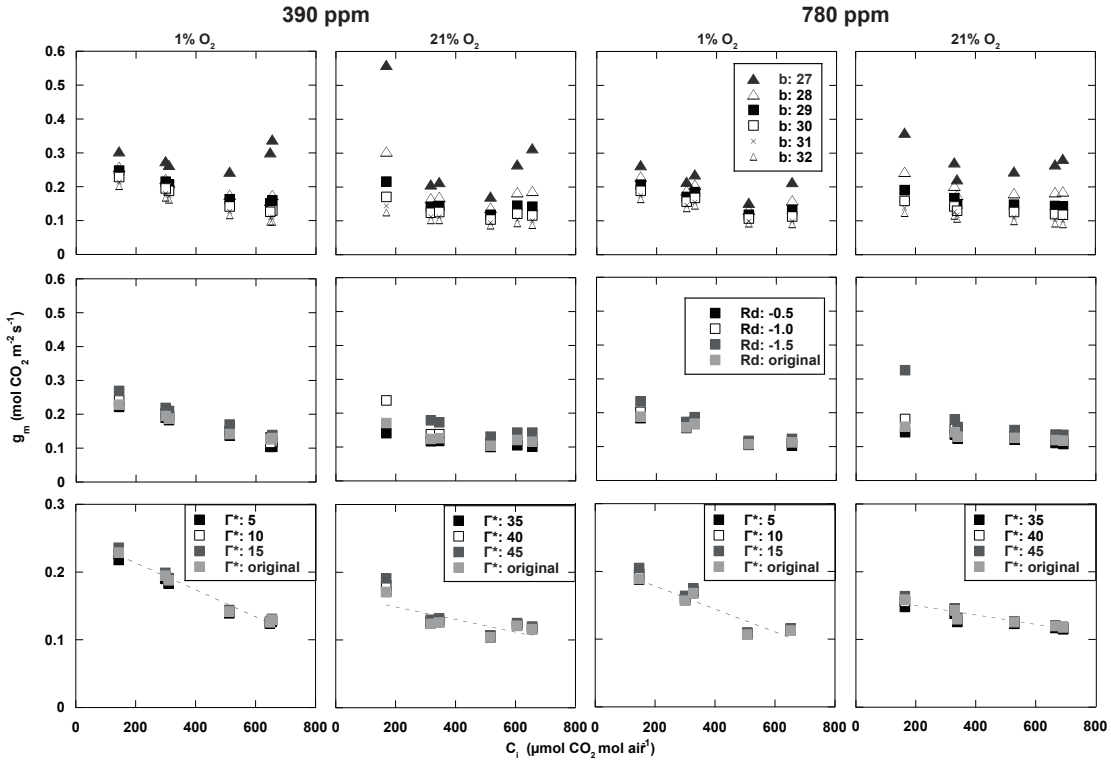

Fig. 6 Sensitivity analyses of g_m to Rubisco fractionation factor b, day respiration (R_d) and CO_2 compesation point (Γ*). The equation of Tazoe *et al.* (2011) was used to calculate g_m. In the bottom figures, regression lines were drawn for the original data, and ANOVA test was performed. Except for the data of plants grown at 390 ppm and measured at 21% O_2, neither of the slopes of these regression lines was zero ($P<0.05$)

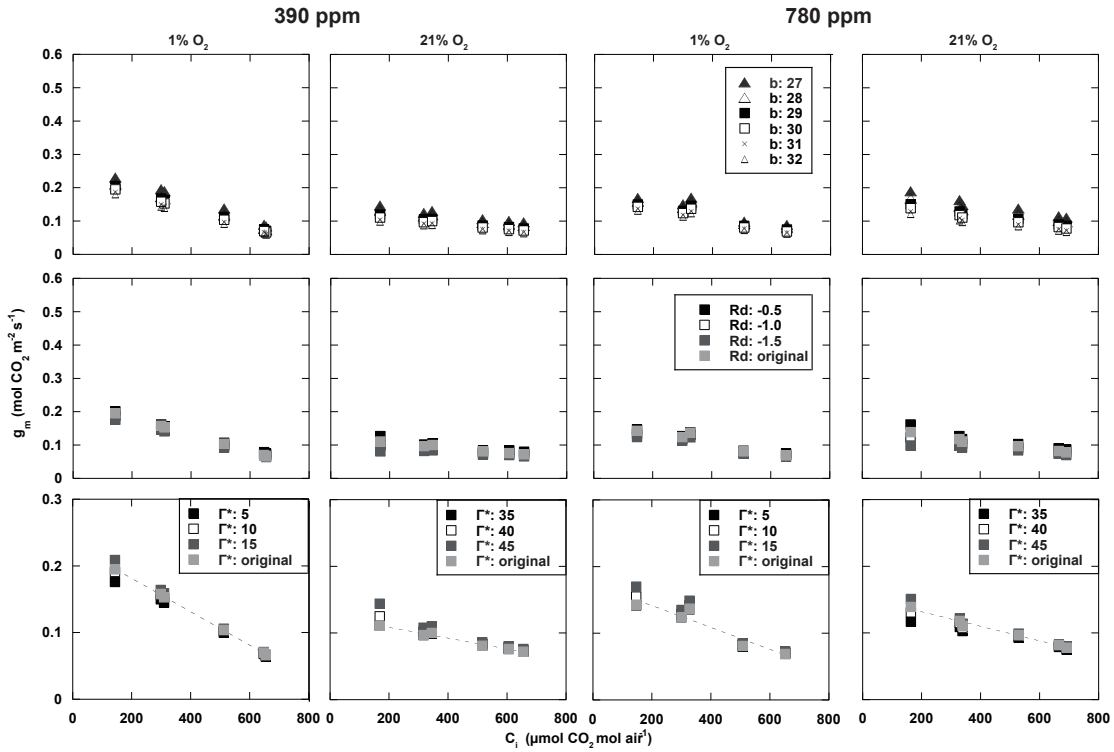

Fig. 7 Sensitivity analyses of g_m to Rubisco fractionation factor b, day respiration (R_d) and CO_2 compesation point (Γ*). The equation of Gu and Sun (2014) was used to calculate g_m In the bottom figures, regression lines were drawn for the original data, and ANOVA test was performed. Neither of the slopes of these regression lines was zero (n=3, P <0.05)

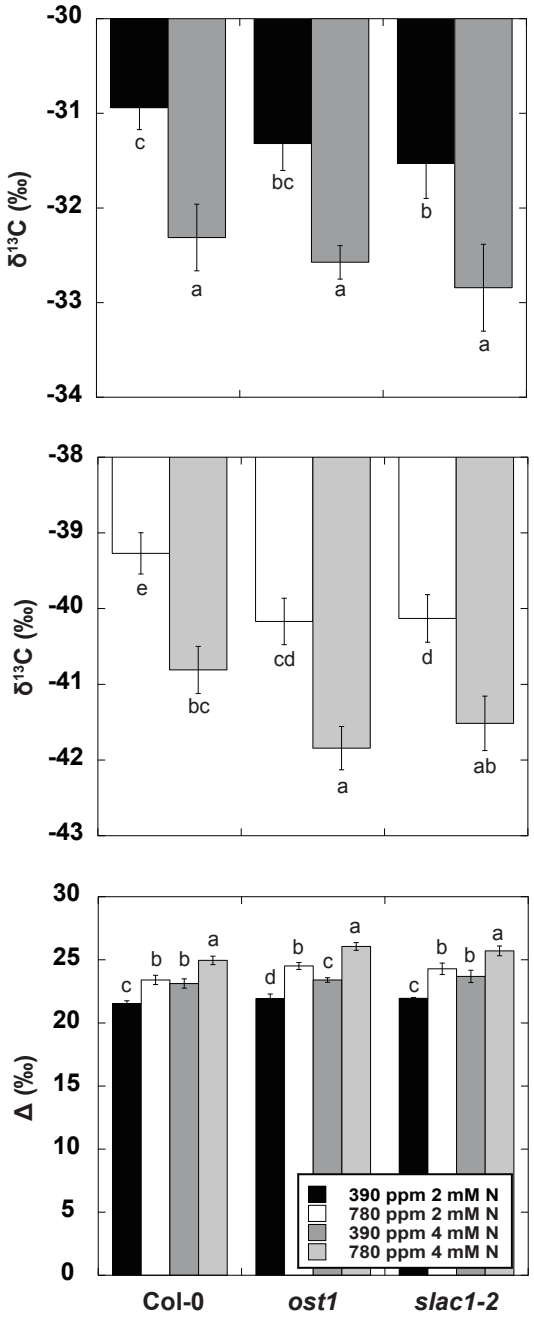

Fig. 8 The comparison of $\delta^{13}C$ and carbon 13 discrimination (Δ) of leaves. The data are mean ± S.D. (n=3-6). Different letters indicated significant differencese (Tukey-HSD, $P < 0.05$).

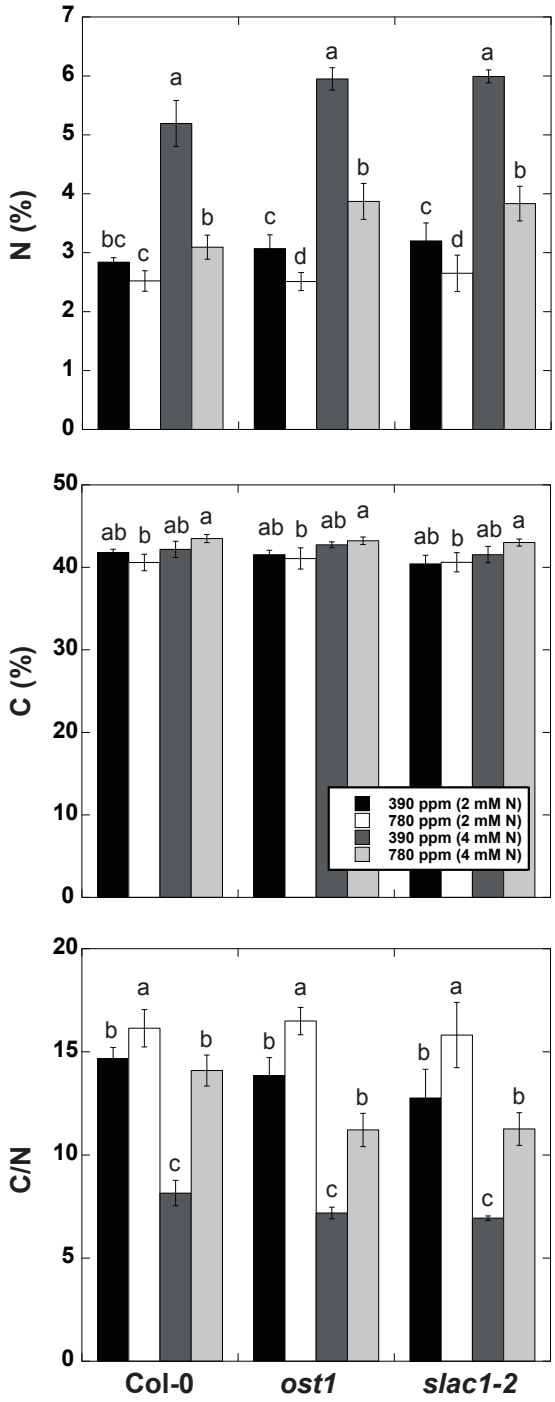

Fig. 9 The comparison of nitrogen content and carbon content of leaf dry matter. Data were mean ± S.D. (Tukey-HSD, $P < 0.05$, n=3-6).

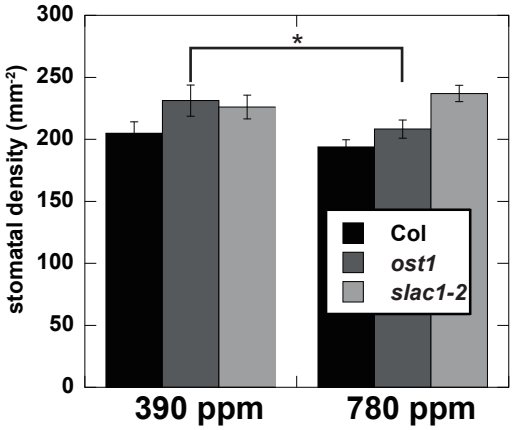

Fig. 10 The comparison of stomatal density among genotypes. The left columns are plants grown at 390 ppm and right colomns are grown at 780 ppm.

Table. 1 Leaf structural traits

		Col-0		*ost1*		*slac1-2*	
		390 ppm	780 ppm	390 ppm	780 ppm	390 ppm	780 ppm
Leaf thickness (μm)	2 mM NO_3^-	209 ± 12	220 ± 11	224 ± 15	215 ± 6	213 ± 12	223 ± 6
	4 mM NO_3^-	250 ± 7 *	254 ± 4 *	277 ± 34	238 ± 15	244 ± 15	250 ± 11
S_m (m^2 m^{-2})	2 mM NO_3^-	9.4 ± 0.3	9.4 ± 0.7	9.4 ± 0.4	9.0 ± 0.3	9.2 ± 0.3	9.6 ± 0.2
	4 mM NO_3^-	9.0 ± 0.3	8.9 ± 0.3	9.4 ± 1.1	8.1 ± 1.0	9.2 ± 0.1	9.6 ± 0.2
S_c (m^2 m^{-2})	2 mM NO_3^-	7.9 ± 0.4	7.8 ± 0.7	7.6 ± 0.5	7.2 ± 0.4	7.5 ± 0.3	8.0 ± 0.2
	4 mM NO_3^-	7.5 ± 0.3	7.7 ± 0.1	8.3 ± 1.0	7.4 ± 0.8	8.2 ± 0.3	6.9 ± 0.5
S_c/S_m (m^2 m^{-2})	2 mM NO_3^-	0.84 ± 0.02	0.83 ± 0.04	0.80 ± 0.04	0.81 ± 0.04	0.82 ± 0.06	0.83 ± 0.01
	4 mM NO_3^-	0.83 ± 0.04	0.86 ± 0.02	0.89 ± 0.01	0.91 ± 0.04	0.90 ± 0.04	0.72 ± 0.06
LMA (g m^{-2})	2 mM NO_3^-	13 ± 1 (c)	23 ± 1 (b)	-	-	-	-
	4 mM NO_3^-	23 ± 3 (b)	33 ± 3 (a)	-	-	-	-

S_m is surface area of mesophyll cells exposed to intercellular air space, S_c is surface area of chloroplast exposed to intercellular air space, and LMA is leaf dry mass per unit leaf area. Gray color represents the data obtained from high nitrogen experiments. Data are mean ± S.E. (n=3-6). Asterisks indicate significant differences (Student's *t*-test, *: $P < 0.05$). Letters indicated significant differences in LMA (Tukey-HSD, $P < 0.05$).

CHAPTER 4

Responses of mesophyll conductance to elevated CO_2 and ABA application in some mutants of *Arabidopsis thaliana*

Introduction

Photosynthetic rate (A) was determined by the photosynthetic capacity and the CO_2 diffusion conductances, i.e., stomatal conductance (g_s) and mesophyll conductance (g_m). g_s responds to various environmental changes such as, drought, light and CO_2 concentration, as well as to application or plant hormones (Assmann *et al.*, 2000, Mott, 2009, Negi *et al.*, 2008, Xue *et al.*, 2011). Under drought conditions, it is reasonable to close stomata to maintain water in the leaves, although it inevitably decreases A, at least in high light, because CO_2 concentration in the chloroplast storoma (C_c) is decreased.

In the case of g_m, however, it has no merit to decrease in g_m in response to environmental changes. However, previous studies have shown that g_m and g_s simultaneously decreased in response to drought and high CO_2 (Flexas *et al.*, 2002, Flexas *et al.*, 2008, Perez-Martin *et al.*, 2014, Tazoe *et al.*, 2011). Therefore, the decrease in g_m was argued to be the secondary effect of the regulation of leaf water relations.

Stomata play an important role in regulation of H_2O and CO_2 fluxes. Therefore, I used *Arabidopsis thaliana* mutants, *slac1-2* and *ost1* already used in the experiment described in CHAPTER 2. Their stomata are deficient in responses to high CO_2 and ABA. In this chapter, I investigated changes in g_m in response to ABA with these mutants.

CO_2 diffuses from the air phase to Rubisco active site via the liquid phase, the latter includes cell wall, plasma membrane, cytosol, chloroplast envelope and stroma.

Recently, many studies have reported that plasma membrane intrinsic protein (PIP), aquaporins, would facilitate CO_2 permeability across the plasma membrane and the chloroplast envelope (Flexas *et al.*, 2006b, Hanba *et al.*, 2004, Heckwolf *et al.*, 2011, Miyazawa *et al.*, 2008, Terashima & Ono, 2002, Uehlein *et al.*, 2003). Aquaporins were first identified as water channels in animal cells (Preston *et al.*, 1992). Since then, functions and regulation mechanisms of aquaporins as water channels have been reported for plant cells (Javot, 2003, Pou *et al.*, 2013, Shatil-Cohen *et al.*, 2011, Tournaire-Roux *et al.*, 2003b, Van Wilder *et al.*, 2008). Moreover, PIP aquaporins regulate leaf water relations in response to environmental changes such as drought, and manipulations such as application of ABA (Boursiac *et al.*, 2008, Pou *et al.*, 2013, Sade *et al.*, 2014, Shatil-Cohen *et al.*, 2011).

PIP aquaporins might be responsible for the decrease in g_m as CO_2 channels or as water channels that change leaf water relations. In *Arabidopsis thaliana*, 13 species of PIP aquaporins are expressed and PIP1;2, PIP2;1, PIP2;3 and PIP2;6 are highly expressed in leaves. Therefore, T-DNA insertion lines of PIP1;2, PIP2;3 and PIP2;6 were used to investigate whether responses of g_m to ABA and high CO_2 were different from wild type.

Materials & Methods

Plant materials

Arabidopsis thaliana and *ost1*, *slac1-2* and T-DNA insertion lines of PIP aquaporins, *pip1;2* (SALK_145347), *pip2;3* (SALK_099862), and *pip2;6* (SALK_029718C) were

grown in 200 mL plastic pots (TERAOKA, Osaka, Japan) containing 1 kg of river sand (SOSEKI, Tochigi, Japan) on the trays in a growth chamber with a 8 h photoperiod, day/night temperature of 23/21℃ and at relative humidity of 60%. Light was provided by fluorescent lamps at photosynthetically active photon flux density (PFD) of 200 μmol photons m^{-2} s^{-1} at leaf level. Fully expanded leaves were used for measurements. *pip1;2* (SALK_145347) and *pip2;3* (SALK_099862) were with a T-DNA insertion within the first intron of PIP1;2 and PIP2;3. *pip2;6* (SALK_029718C) was with a T-DNA insertion within the third intron of PIP2;6.

Measurement conditions of g_m

To investigate the g_m responses to ABA, Col-0, *ost1* and *slac1-2* were fed with 20 μM ABA solution via slits in the petioles. When ABA solution was applied from the petiole of the cut leaf, *ost1* and *slac1-2* tended to wilt in about 1 h probably because they were open-stomata phenotypes. Therefore, I peeled the epidermis of the midrib and made a slit with a razor blade and added ABA solution to the slit. ABA solution was prepared with an artificial xylem sap (AXS) containing 1 mM K- phosphate buffer (pH 5.8), 1 mM $CaCl_2$, 0.1 mM $MgSO_4$, 3 mM KNO_3 and 0.1 mM $MnSO_4$ (Wilkinson & Davies, 1997).The plant from a growth chamber was kept in the dark for more than 15 min to avoid embolism before and during making the slit. After making a slit, control solution (ABA free AXS) was applied and the leaf was enclosed in the chamber. Light at PFD of 600 μmol m^{-2} s^{-1} was provided by a metal halide lamp (PCS-UMX250; NPI, Tokyo, Japan). The rate of photosynthesis was measured at an ambient CO_2 concentration (C_a)

of 390 μmol mol^{-1} and O_2 concentration of 1%. The leaf temperature was kept at 22°C and the leaf to air vapor pressure deficit (VPD) was set to 0.65 ± 0.1 kPa. Gas exchange parameters were calculated according to von Caemmerer & Farquhar (1981). When leaf photosynthesis attained a steady-state rate, photosynthetic characteristics were measured, and an ABA solution was applied. Photosynthetic characteristics were measured after 1.5 h of the application of the ABA solution.

Leaves of the PIP mutants were cut at their petioles in the deionized water and kept in 1.5 mL micro tubes. The deionized water in micro tube was replaced with AXS, and measurements were made after the photosynthesis rate attained a steady-state rate. The AXS in the micro tube was then replaced with an AXS containing 1 μM ABA, and made measurements in 1.5 h.

All the measurements for elevated CO_2 experiments were conducted at 390 ppm at first, and then CO_2 concentration was elevated to 780 ppm, and made measurements in 1.5 h.

Calculation of mesophyll conductance and measurement of ABA content in leaves

The mesophyll conductance was calculated by the same method as in CHAPTER 2. Parameters used in this study were the same as in CHAPTER 3.

The measurements of ABA content in the leaves were based on the method as described in CHAPTER2. In CHAPTER4, two leaves were used for the measurement.

Results

In Fig. 1, data are expressed as relative values where the values before the ABA treatment were set to one. The photosynthetic rate (A) in Col-0 decreased after application of ABA, and A in *slac1-2* also slightly decreased. g_s decreased in response to application of ABA in Col-0 and *slac1-2*, On the other hand, g_s was almost insensitive to ABA in *ost1*. g_m was apparently decreased after ABA application even data calculated with the method of Gu and Sun (2014) in Col-0. g_m in *slac1-2* did not decrease to the same level of that in Col-0. g_m in *ost1* was insensitive to ABA. When the ABA content in the leave was plotted against g_s, g_m and g_m calculated with the method of Gu & Sun (2014), g_s was more sensitive to ABA than g_m (Fig. 2). In addition, ABA content before ABA application in *ost1* and *slac1-2* was greater than that in Col-0.

The experiments using PIP T-DNA insertion lines showed that the photosynthetic characteristics of these lines were very similar (Fig. 3). Responses of photosynthetic characteristics to the elevated CO_2 and ABA were expressed as relative values. In all lines, responses in g_m to elevated CO_2 were similar (Fig. 4). On the other hand, responses in g_m to ABA were different among the lines. g_m in *pip2;6* was slightly greater than that in Col-0 after ABA application (Fig. 5).

Discussion

Application of 20 μM ABA resulted in large decreases in g_s and g_m in Col-0 (Fig. 1). On the other hand, g_s decreased only slightly and g_m was almost insensitive in response

to ABA in *slac1-2*. Decrease in g_s in *slac1-2* could be explained by activation of another anion channel, QUAC1(Imes *et al.*, 2013). These independent responses of g_s and g_m implied that decrease in g_s was not necessarily linked with the decrease in g_m. Previous studies have reported simultaneous decrease in g_s and g_m and discussed about a possible involvement of lowered g_s on g_m (Flexas *et al.*, 2009, Flexas *et al.*, 2002, Flexas *et al.*, 2008). Lowered g_s might increase the influences of CO_2 from respiration and photorespiration because incoming CO_2 flow from outside of the leaves are restricted. In this study, measurements were conducted at 1% O_2 condition to minimize the effect of photorespiration. Moreover, the method incorporated the effects of respired and photorespired CO_2 was also used to estimate g_m, but g_m decreased consistently. Therefore, the decrease in g_m in response to ABA was due to neither the effect of (photo)respired CO_2 nor that of the decrease in g_s. Then, another question arises because, in *slac1-2* and *ost1*, g_m was not decreased by ABA application. OST1 is a protein kinase that mediates stomatal closure in response to elevated CO_2 or ABA (Xue *et al.*, 2011). OST1 kinase activates SLAC1 via phosphorylation (Imes *et al.*, 2013, Xue *et al.*, 2011). Possible explanations are discussed below with the results of the experiments with PIP aquaporins T-DNA insertion lines.

In analyses of g_m in response to elevated CO_2 and ABA with PIP T-DNA insertion lines, photosynthetic characteristics in all lines were similar (Fig. 3). However, previous studies have reported that *pip1;2* had lower A and g_m (Heckwolf *et al.*, 2011, Uehlein *et al.*, 2012). These results from the same group might be due to difference line of seeds

because other researchers could not reproduce these results (Professor Bernerd Genty, personal communication).

Responses of g_m to ABA in *pip2;6* were smaller than those in Col-0. PIP2;6 was mainly expressed around vascular tissue (Prado *et al.*, 2013), therefore they would not play a role in mesophyll cells as CO_2 facilitators (Fig. 5). Recently, the positive relationships between g_m and leaf water relations have been reported (Ferrio *et al.*, 2012, Flexas *et al.*, 2012). In addition, ABA decreased water permeability of bundle sheath cells via regulation of PIP aquaporins (Sade *et al.*, 2014, Shatil-Cohen *et al.*, 2011). When these reports were taken into consideration, the increase in ABA content in the leaf, specifically in xylem sap, decreased water permeability via PIP aquaporins, and affected water relations that would then decrease g_m. In CHAPTER 2, tobacco plants exposed to drought conditions showed decreases in leaf water potential and g_m. This data also supports this idea. These changes in water relations via PIP aquaporins might be regulated with phosphorylation of PIP aquaporins. In the root cells, salinity affected phosphorylation state of C-terminal tail of PIP2;1 and changed subcellular localization of PIP2;1 as intercellular compartments (Prak *et al.*, 2008).

Considering the insensitivity of g_m to ABA in *slac1-2* and *ost1*, I might suggest a possible explanation of their insensitivity in g_m from the point of view of water relations. At first, they had greater g_s than Col-0. Therefore, their water relations might differ from those of Col-0, because the plants of *Arabidopsis thaliana* having greater g_s tend to have lower leaf water potential than that with lower g_s (Pantin *et al.*, 2013). Moreover, they, especially *slac1-2*, had slightly smaller g_m than Col-0, when measurements were

conducted at 390 ppm and 1% O_2 in CHAPTER 3. This might be due to changes in water relations. Interestingly, OST1 is expressed at both stomata and leaf vascular tissues (Mustilli, 2002). Therefore, they would control leaf water relations by changing water permeability around bundle sheath cells and closing stomata. These two regulations are important to determine leaf water potential. As I have already mentioned above, phosphorylation state of PIP aquaporins affects water permeability. Then, OST1 would be one of the candidates to change phosphorylation state of PIP aquaporins in the bundle sheath cells. If the leaf water relations are closely related to g_m, these changes in water relations might alter the response of g_m to ABA.

In this study, I suggested the possible involvement of PIP aquaporins in regulation of g_m in response to ABA through changing water relations of leaves. Previous reports have demonstrated that the relationships between leaf water relations and PIP aquaporins, and those of leaf water relations and g_m. However, there is no report that demonstrates g_m is regulated with leaf water relations that are regulated by PIP aquaporins. Further investigations are needed to elucidate the mechanisms of g_m regulation in response to ABA.

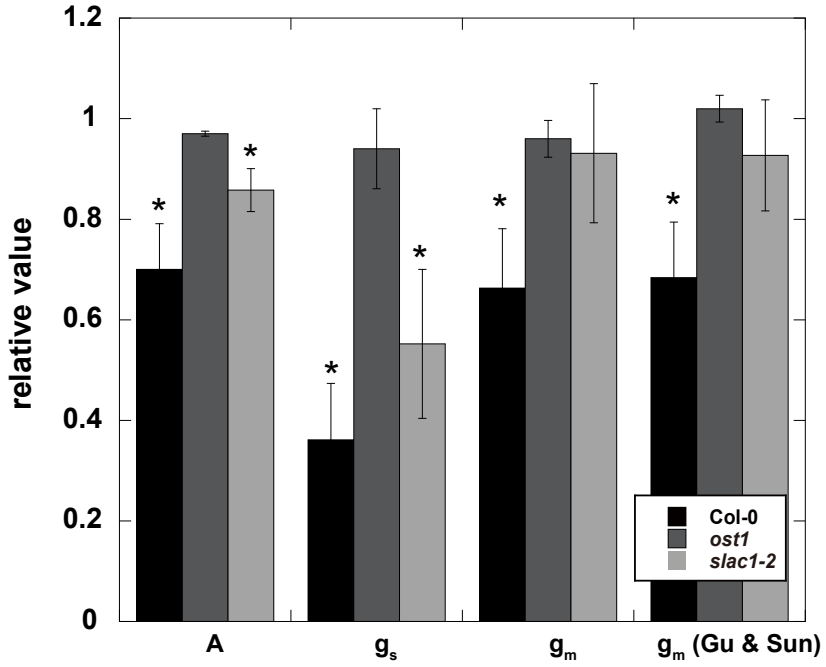

Fig. 1 Changes of photosynthetic characteristics after 20 μM ABA application. The vales were expressed as relative values when the values before ABA application set to one. Data were mean ± S.D. (n=3-5). Asterisks indicate the significant differences between before ABA application and after the treatment (Student-*t* test, $P<0.05$).

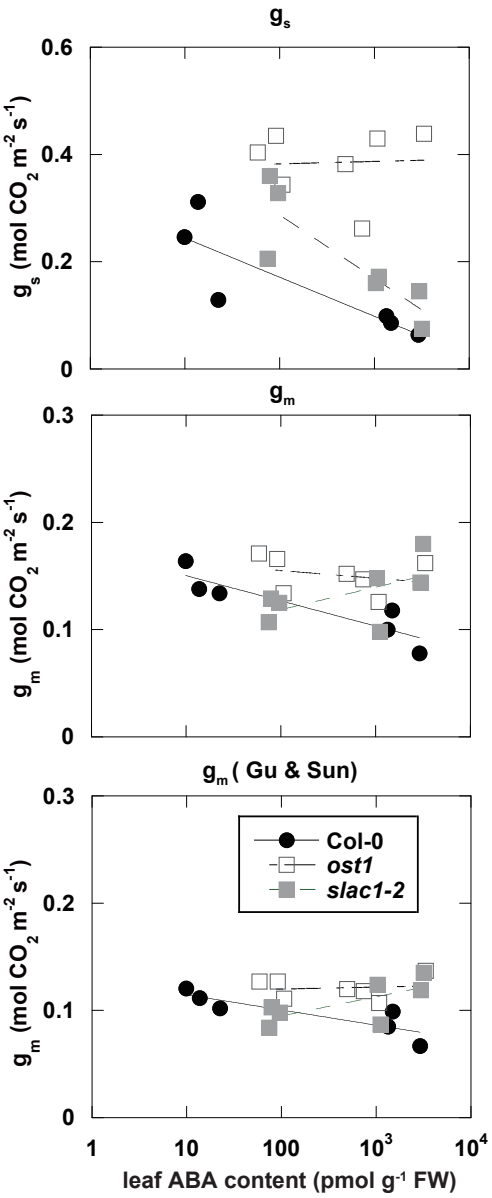

Fig. 2 The relationships among CO_2 diffusion conductances and ABA content in leaves. In this figure, control values were from another batch of experiment, therefore control values were different from value used in Fig. 1.

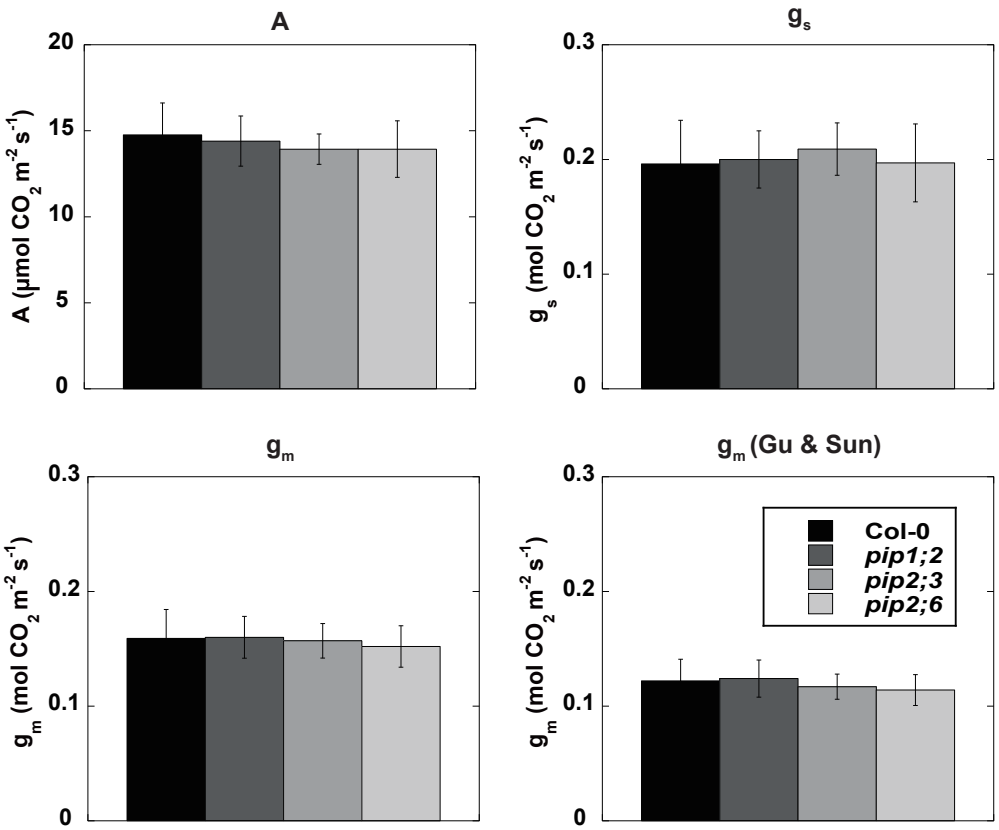

Fig. 3 Comparison of photosynthetic characteristics among Col-0 and PIP T-DNA insertion lines. Data were mean ± S.D. (n=3-6).

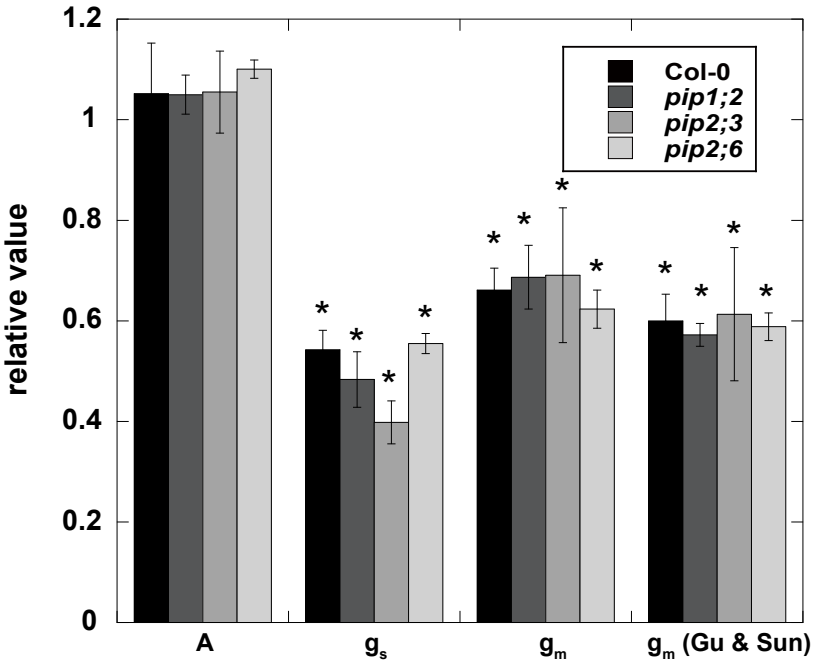

Fig. 4 Changes of photosynthetic characteristics after elevation of CO_2 concentration. The vales were expressed as relative values when the values at CO_2 concentration of 390 ppm set to one. Data were mean ± S.D. (n=3). Asterisks indicate the significant differences between control and after the treatment (Student-*t* test, $P<0.05$).

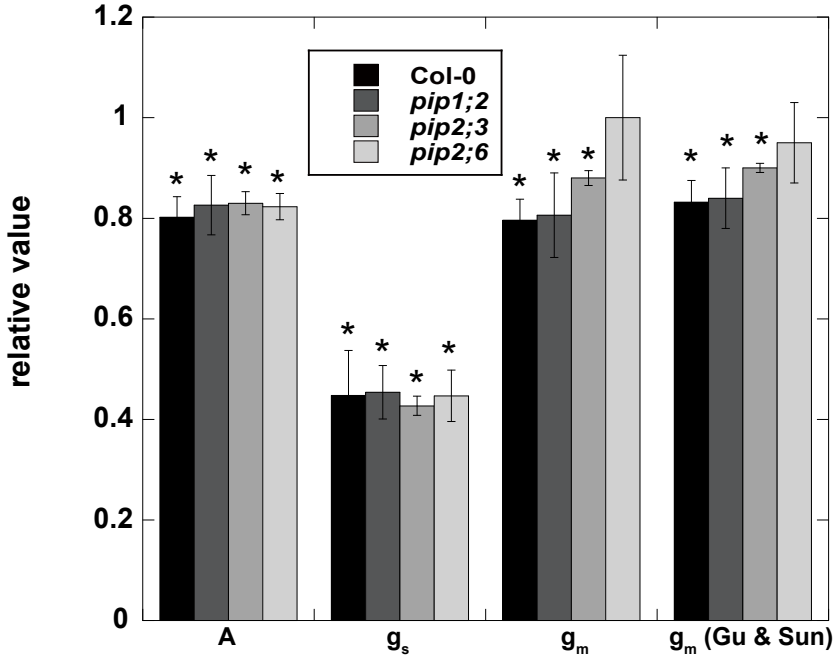

Fig. 5 Changes of photosynthetic characteristics after 1 μM ABA application. The values were expressed as relative values when the values before ABA application set to one. Data were mean ± S.D. (n=4-6). Asterisks indicate the significant differences between before ABA application and after the treatment (Student-*t* test, $P<0.05$).

CHAPTER 5

General discussion

Method for estimating g_m

The methods for estimating g_m have been improving and I mentioned and discussed the related methodological problems in Chpaters 1, 2 and 3. Previous studies have already suggested the method for estimating g_m should be accurate and the method with the minimum assumptions should be used to obtain the data with high accuracy (Pons *et al.*, 2009). However, many studies have used the chlorophyll fluorescence method with less attention to the important parameters that are needed for the calculation of g_m, as pointed out recently (Gu & Sun, 2014). Whenever the responses of g_m to environmental changes are important, the methods for estimating g_m and measurement conditions have to be carefully considered.

In the present study, the carbon isotope method with high accuracy has been used with two calculation methods described in CHAPTER 3 (Gu & Sun, 2014, Tazoe *et al.*, 2011). The method used by Tazoe *et al.* (2011) does not take into account the re-fixation of CO_2 from mitochondria. Gu and Sun (2014) have improved the equations to incorporate the re-fixation of the CO_2. When the data were re-calculated with the method of Gu and Sun (2014), the values of g_m slightly smaller than those calculated with Tazoe *et al.* (2011). However, the results in CHAPTER 3 and 4 showed that the responses of g_m to CO_2 and ABA were consistently observed by both methods. The difference in g_m by these methods was about 0.03 mol CO_2 m^{-2} s^{-1}, and the difference in g_m resulted in the difference in C_c of about 26 μmol CO_2 mol air^{-1} in high light at the ambient CO_2 condition at 390 ppm in Col-0.

At present, the method proposed by Gu and Sun (2014) for estimating g_m is most advanced, but their method also has many assumptions. Therefore, a more direct method should be sought. Nevertheless, when carefully used with relevant sensitivity analyses, their method would produce reliable g_m values.

Responses of g_m to C_i and ABA

It was revealed that the decrease in g_m in response to elevated CO_2 and the decrease in g_m in response to ABA were brought about by the different mechanisms. When the leaf was subject to elevated CO_2, C_i increased, while C_i was decreased with application of ABA. In both cases, g_m was decreased. In other words, the increase in g_m was not observed when ABA was applied although C_i decreased. Further, experiments with ABA deficient tobacco have revealed that ABA is not necessary for decreasing g_m in response to high CO_2.

The rapid decrease in g_m in response to elevated CO_2 could be explained by leakiness of the chloroplast envelope to HCO_3^-. However, when the plants grown at high N, the responses of g_m to high CO_2 changed considerably, and these changes would not be explained by the leakiness alone. These changes might be due to changes in the chloroplast thickness and its content. Basically, when chloroplast becomes bigger, the diffusion pathlength to Rubisco in the stroma becomes larger, and thereby g_m would decrease. The chloroplast size may be changed by the nitrogen nutrition level and growth CO_2 concentration because growth at low N and/or high CO_2

leads the leaves to accumulate much starch. Then, the chloroplast will become thicker. Moreover, the stroma includes large barriers for CO_2 and HCO_3^- diffusion.

Possible factors altering g_m under drought condition

In CHAPTER 2, I demonstrated the involvement of ABA in the decrease in g_m. ABA plays an important role under drought conditions in leaf water relations. With respect to the decrease in g_m in response to ABA, it is possible that the decrease in g_m is the secondary effect of the changes in leaf hydraulics. There are two possible explanations for that.

One of them is direct regulation of PIP aquaporins. Recently, many studies have reported that some PIP aquaporins have ability to permeate CO_2 (Flexas *et al.*, 2006b, Hanba *et al.*, 2004, Mori *et al.*, 2014, Uehlein *et al.*, 2003). PIP aquaporins exist in the plasma membrane as heterotetramers and these interactions of PIP aquaporins regulate their localization (Otto *et al.*, 2010, Zelazny *et al.*, 2007). A previous study demonstrated that inactivation of PIP aquaporins under drought condition occurred by conformational changes via dephosphorylation (Tornroth-Horsefield *et al.*, 2006). When the four PIP aquaporins exist as a heterotetramer in the plasma membrane, and one of them is the CO_2 facilitator and the others are water channels, inactivation of water permeable PIP aquaporins under drought conditions might change the conformation of the heterotetramer. In short, it might be possible that the CO_2 permeable PIP aquaporin is also inactivated by regulation of the water permeable PIP aquaporins. It might be also possible that the heterotetramer PIP aquaporins change its localization as intracellular

compartments. This trafficking regulation of PIP aquaporins has been demonstrated in root cells under salt stress (Luu *et al.*, 2012, Prak *et al.*, 2008). If the water permeable and CO_2 permeable PIP aquaporins form heterotetramer together in the plasma membrane in the mesophyll cells. The effect of regulating water relations in mesophyll cells could result in the decrease in g_m as well.

Another explanation of the decrease in g_m in response to ABA is indirect involvement of PIP aquaporins. There is a significant resistance for water between xylem and bundle sheath cells, and this resistance is partly regulated by PIP aquaporins (Sade *et al.*, 2014, Shatil-Cohen *et al.*, 2011). In their studies, application of ABA decreased the water permeability of bundle sheath cells, and then decreased water conductivity of the leaves and leaf water potential. In the present study, the decrease in water potential of tobacco leaves was observed under the drought conditions. In this way, leaf water relations are correlated with g_m as suggested by Ferrio *et al.* (2012). Therefore, ABA might affect leaf water relations and thereby the decrease g_m via PIP aquaporin regulation.

Future perspectives

The involvement of ABA in the decrease in g_m under drought conditions is proposed. However, underlying mechanisms of decrease in g_m is still unclear. As a mechanism that decreases g_m, the role of ABA in regulation of the leaf water relations is suggested. It is possible to investigate this hypothesis. Clarification of the relationships between leaf water relations and CO_2 diffusion in the leaves will be important to improve

crops that have high photosynthesis rate with less water. Detailed analyses of responses of CO_2 diffusion conductances to high CO_2 will be helpful to improve plants performance. Currently, the atmospheric CO_2 concentration is increasing dramatically. Therefore, we should seriously consider the consequences of the increase in the atmospheric CO_2. At the same time, we should consider how we improve plant performance in such the high CO_2 world. If my study is regarded as one of the pioneering studies in this research field, my efforts will be rewarded.

References

Ainsworth E.A. & Long S.P. (2005) What have we learned from 15 years of free-air CO_2 enrichment (FACE)? A meta-analytic review of the responses of photosynthesis, canopy properties and plant production to rising CO_2. *New Phytol*, **165**, 351-371.

Ainsworth E.A. & Rogers A. (2007) The response of photosynthesis and stomatal conductance to rising [CO_2]: mechanisms and environmental interactions. *Plant Cell Environ*, **30**, 258-270.

Araya T., Noguchi K. & Terashima I. (2006) Effects of carbohydrate accumulation on photosynthesis differ between sink and source leaves of *Phaseolus vulgaris* L. *Plant Cell Physiol*, **47**, 644-652.

Assmann S.M., Snyder J.A. & Lee Y.R.J. (2000) ABA−deficient (*aba1*) and ABA−insensitive (*abi1−1*, *abi2−1*) mutants of Arabidopsis have a wild-type stomatal response to humidity. *Plant Cell Environ*, **23**, 387-395

Bauer H., Ache P., Lautner S., Fromm J., Hartung W., Al-Rasheid K.A., Sonnewald S., Sonnewald U., Kneitz S., Lachmann N., Mendel R.R., Bittner F., Hetherington A.M. & Hedrich R. (2013) The stomatal response to reduced relative humidity requires guard cell-autonomous ABA synthesis. *Curr Biol*, **23**, 53-57.

Bernacchi C.J., Morgan P.B., Ort D.R. & Long S.P. (2005) The growth of soybean under free air [CO_2] enrichment (FACE) stimulates photosynthesis while decreasing in vivo Rubisco capacity. *Planta*, **220**, 434-446.

Boursiac Y., Boudet J., Postaire O., Luu D.T., Tournaire-Roux C. & Maurel C. (2008) Stimulus-induced downregulation of root water transport involves

reactive oxygen species-activated cell signalling and plasma membrane intrinsic protein internalization. *Plant J*, **56**, 207-218.

Boyer J.S., Wong S.C. & Farquhar G.D. (1997) CO_2 and water vapor exchange across leaf cuticle (epidermis) at various water potentials. *Plant Physiol*, **114**, 185-191.

Bunce J.A. (1998) Effects of humidity on short−term responses of stomatal conductance to an increase in carbon dioxide concentration. *Plant Cell Environ*, **21**, 115-120.

Bunce J.A. (2002) Sensitivity of infrared water vapor analyzers to oxygen concentration and errors in stomatal conductance. *Photosynthesis Research*, **71**, 273-276.

Caemmerer S.V. & Evans J.R. (1991) Determination of the average partial pressure of CO_2 in chloroplasts from leaves of several C_3 plants. *Functional Plant Biology*, **18**, 287-305.

Canny M., Wong S.C., Huang C. & Miller C. (2012) Differential shrinkage of mesophyll cells in transpiring cotton leaves: implications for static and dynamic pools of water, and for water transport pathways. *Functional Plant Biology*, **39**, 91-102.

Christmann A., Weiler E.W., Steudle E. & Grill E. (2007) A hydraulic signal in root-to-shoot signalling of water shortage. *Plant J*, **52**, 167-174.

Delfine S., Loreto F., Pinelli P., Tognetti R. & Alvino A. (2005) Isoprenoids content and photosynthetic limitations in rosemary and spearmint plants under water stress. *Agriculture, Ecosystems & Environment*, **106**, 243-252.

Douthe C., Dreyer E., Epron D. & Warren C.R. (2011) Mesophyll conductance to

CO_2, assessed from online TDL-AS records of $^{13}CO_2$ discrimination, displays small but significant short-term responses to CO_2 and irradiance in Eucalyptus seedlings. *J Exp Bot*, **62**, 5335-5346.

Endo A., Sawada Y., Takahashi H., Okamoto M., Ikegami K., Koiwai H., Seo M., Toyomasu T., Mitsuhashi W., Shinozaki K., Nakazono M., Kamiya Y., Koshiba T. & Nambara E. (2008) Drought induction of Arabidopsis 9-cis-epoxycarotenoid dioxygenase occurs in vascular parenchyma cells. *Plant Physiol*, **147**, 1984-1993.

Ethier G.J. & Livingston N.J. (2004) On the need to incorporate sensitivity to CO_2 transfer conductance into the Farquhar–von Caemmerer–Berry leaf photosynthesis model. *Plant Cell Environ*, **27**, 137-153.

Evans J., Sharkey T., Berry J. & Farquhar G. (1986) Carbon isotope discrimination measured concurrently with gas exchange to investigate CO_2 diffusion in leaves of higher plants. *Functional Plant Biology*, **13**, 281-292.

Evans J.R. (1983) Nitrogen and photosynthesis in the flag leaf of wheat (*Triticum aestivum* L.). *Plant Physiol*, **72**, 297-302.

Evans J.R., Caemmerer S.V., Setchell B.A. & Hudson G.S. (1994) The relationship between CO_2 transfer conductance and leaf anatomy in transgenic tobacco with a reduced content of Rubisco. *Functional Plant Biology*, **21**, 475-495.

Fabre N., Reiter I.M., Becuwe-Linka N., Genty B. & Rumeau D. (2007) Characterization and expression analysis of genes encoding alpha and beta carbonic anhydrases in Arabidopsis. *Plant Cell Environ*, **30**, 617-629.

Farquhar G., von Caemmerer S.v. & Berry J. (1980) A biochemical model of

photosynthetic CO_2 assimilation in leaves of C_3 species. *Planta*, **149**, 78-90.

Farquhar G.D. & Cernusak L.A. (2012) Ternary effects on the gas exchange of isotopologues of carbon dioxide. *Plant Cell Environ*, **35**, 1221-1231.

Farquhar G.D., Ehleringer J.R. & Hubick K.T. (1989) Carbon isotope discrimination and photosynthesis. *Annual Review of Plant Biology*, **40**, 503-537.

Ferrio J.P., Pou A., Florez-Sarasa I., Gessler A., Kodama N., Flexas J. & Ribas-Carbo M. (2012) The Peclet effect on leaf water enrichment correlates with leaf hydraulic conductance and mesophyll conductance for CO_2. *Plant Cell Environ*, **35**, 611-625.

Flexas J., Barbour M.M., Brendel O., Cabrera H.M., Carriqui M., Diaz-Espejo A., Douthe C., Dreyer E., Ferrio J.P., Gago J., Galle A., Galmes J., Kodama N., Medrano H., Niinemets U., Peguero-Pina J.J., Pou A., Ribas-Carbo M., Tomas M., Tosens T. & Warren C.R. (2012) Mesophyll diffusion conductance to CO_2: an unappreciated central player in photosynthesis. *Plant Sci*, **193-194**, 70-84.

Flexas J., Baron M., Bota J., Ducruet J.M., Galle A., Galmes J., Jimenez M., Pou A., Ribas-Carbo M., Sajnani C., Tomas M. & Medrano H. (2009) Photosynthesis limitations during water stress acclimation and recovery in the drought-adapted *Vitis* hybrid Richter-110 (*V. berlandierixV. rupestris*). *J Exp Bot*, **60**, 2361-2377.

Flexas J., Bota J., Escalona J.M., Sampol B. & Medrano H. (2002) Effects of drought on photosynthesis in grapevines under field conditions: an evaluation of stomatal and mesophyll limitations. *Functional Plant Biology*, **29**, 461-471.

Flexas J., Diaz-Espejo A., Galmes J., Kaldenhoff R., Medrano H. & Ribas-Carbo M. (2007a) Rapid variations of mesophyll conductance in response to changes in CO2 concentration around leaves. *Plant Cell Environ*, **30**, 1284-1298.

Flexas J., DIAZ‐ESPEJO A., GalmES J., Kaldenhoff R., Medrano H. & RIBAS‐CARBO M. (2007b) Rapid variations of mesophyll conductance in response to changes in CO_2 concentration around leaves. *Plant Cell Environ*, **30**, 1284-1298.

Flexas J., Ribas-Carbo M., Bota J., Galmes J., Henkle M., Martinez-Canellas S. & Medrano H. (2006a) Decreased Rubisco activity during water stress is not induced by decreased relative water content but related to conditions of low stomatal conductance and chloroplast CO_2 concentration. *New Phytol*, **172**, 73-82.

Flexas J., Ribas-Carbo M., Diaz-Espejo A., Galmes J. & Medrano H. (2008) Mesophyll conductance to CO_2: current knowledge and future prospects. *Plant Cell Environ*, **31**, 602-621.

Flexas J., Ribas-Carbo M., Hanson D.T., Bota J., Otto B., Cifre J., McDowell N., Medrano H. & Kaldenhoff R. (2006b) Tobacco aquaporin NtAQP1 is involved in mesophyll conductance to CO_2 in vivo. *Plant J*, **48**, 427-439.

Gaastra P. (1959) *Photosynthesis of crop plants as influenced by light, carbon dioxide, temperature, and stomatal diffusion resistance*. H. Veenman en Zonen N. v.

Galle A., Florez-Sarasa I., Tomas M., Pou A., Medrano H., Ribas-Carbo M. & Flexas J. (2009) The role of mesophyll conductance during water stress and recovery in tobacco (Nicotiana sylvestris): acclimation or limitation? *J Exp Bot*, **60**, 2379-2390.

Galmes J., Medrano H. & Flexas J. (2007) Photosynthetic limitations in response to water stress and recovery in Mediterranean plants with different growth forms. *New Phytol*, **175**, 81-93.

Genty B., Briantais J.-M. & Baker N.R. (1989) The relationship between the quantum yield of photosynthetic electron transport and quenching of chlorophyll fluorescence. *Biochimica et Biophysica Acta (BBA)-General Subjects*, **990**, 87-92.

Genty B., Meyer. S., Piel C.C.F. & Liozon R. (1998) CO_2 diffusion inside leaf mesophyll of ligneous plants. *Kluwer Academic Publishers*, 3961-3966.

Gu L. & Sun Y. (2014) Artefactual responses of mesophyll conductance to CO_2 and irradiance estimated with the variable J and online isotope discrimination methods. *Plant Cell Environ*, **37**, 1231-1249.

Hanba Y.T., Shibasaka M., Hayashi Y., Hayakawa T., Kasamo K., Terashima I. & Katsuhara M. (2004) Overexpression of the barley aquaporin HvPIP2; 1 increases internal CO_2 conductance and CO_2 assimilation in the leaves of transgenic rice plants. *Plant and Cell Physiology*, **45**, 521-529.

Harley P.C., Loreto F., Di Marco G. & Sharkey T.D. (1992) Theoretical considerations when estimating the mesophyll conductance to CO_2 flux by analysis of the response of photosynthesis to CO2. *Plant Physiol*, **98**, 1429-1436.

Hashimoto-Sugimoto M., Higaki T., Yaeno T., Nagami A., Irie M., Fujimi M., Miyamoto M., Akita K., Negi J., Shirasu K., Hasezawa S. & Iba K. (2013) A Munc13-like protein in Arabidopsis mediates H+-ATPase translocation that is essential for stomatal responses. *Nat Commun*, **4**, 2215.

Heckwolf M., Pater D., Hanson D.T. & Kaldenhoff R. (2011) The *Arabidopsis* thaliana aquaporin AtPIP1;2 is a physiologically relevant CO_2 transport

facilitator. *Plant J*, **67**, 795-804.

Imes D., Mumm P., Bohm J., Al-Rasheid K.A., Marten I., Geiger D. & Hedrich R. (2013) Open stomata 1 (OST1) kinase controls R-type anion channel QUAC1 in Arabidopsis guard cells. *Plant J*, **74**, 372-382.

Javot H. (2003) Role of a Single Aquaporin Isoform in Root Water Uptake. *The Plant Cell Online*, **15**, 509-522.

Kariya K.T., S. (1972) Relationships of chlorophyll content, chloroplast area index and leaf photosynthesis rate in Brassica. *Tohoku Journal of Agricultural Research*, **23**, 1-14.

Kogami H., Hanba Y., Kibe T., Terashima I. & Masuzawa T. (2001) CO_2 transfer conductance, leaf structure and carbon isotope composition of *Polygonum cuspidatum* leaves from low and high altitudes. *Plant Cell Environ*, **24**, 529-538.

Kojima M., Kamada-Nobusada T., Komatsu H., Takei K., Kuroha T., Mizutani M., Ashikari M., Ueguchi-Tanaka M., Matsuoka M., Suzuki K. & Sakakibara H. (2009) Highly sensitive and high-throughput analysis of plant hormones using MS-probe modification and liquid chromatography-tandem mass spectrometry: an application for hormone profiling in Oryza sativa. *Plant Cell Physiol*, **50**, 1201-1214.

Kuromori T., Miyaji T., Yabuuchi H., Shimizu H., Sugimoto E., Kamiya A., Moriyama Y. & Shinozaki K. (2010) ABC transporter AtABCG25 is involved in abscisic acid transport and responses. *Proc Natl Acad Sci U S A*, **107**, 2361-2366.

Laing W.A., Ogren W.L. & Hageman R.H. (1974) Regulation of soybean net photosynthetic CO_2 fixation by the interaction of CO_2, O_2, and ribulose 1, 5-diphosphate carboxylase. *Plant Physiol*, **54**, 678-685.

Laisk A.K. (1977) Kinetics of photosynthesis and photorespiration of C_3 in plants.

Laisk A.O., M. Rahi. (1970) Diffusion resistances as related to the leaf anatomy. *Fiziologiya Rastenii*, **17**, 40-48.

Lanigan G.J., Betson N., Griffiths H. & Seibt U. (2008) Carbon isotope fractionation during photorespiration and carboxylation in Senecio. *Plant Physiol*, **148**, 2013-2020.

Leakey A.D., Xu F., Gillespie K.M., McGrath J.M., Ainsworth E.A. & Ort D.R. (2009) Genomic basis for stimulated respiration by plants growing under elevated carbon dioxide. *Proc Natl Acad Sci U S A*, **106**, 3597-3602.

Leydecker M.-T., Moureaux T., Kraepiel Y., Schnorr K. & Caboche M. (1995) Molybdenum cofactor mutants, specifically impaired in xanthine dehydrogenase activity and abscisic acid biosynthesis, simultaneously overexpress nitrate reductase. *Plant Physiol*, **107**, 1427-1431.

Luu D.T., Martiniere A., Sorieul M., Runions J. & Maurel C. (2012) Fluorescence recovery after photobleaching reveals high cycling dynamics of plasma membrane aquaporins in Arabidopsis roots under salt stress. *Plant J*, **69**, 894-905.

Makino A., Mae T. & Ohira K. (1986) Colorimetric Mwasurement of Protein Stained with Coomassie Brilliant Blue R on Sodium Dodecyl Sulfate-Polyacrylamide Gel Electrophoresis by Eluting with Formamide. *Agric. Biol. Chem*, **50**, 1911-1912.

McAdam S.A. & Brodribb T.J. (2012) Fern and lycophyte guard cells do not respond to endogenous abscisic acid. *Plant Cell*, **24**, 1510-1521.

Miyazawa S.-I., Yoshimura S., Shinzaki Y., Maeshima M. & Miyake C. (2008) Deactivation of aquaporins decreases internal conductance to CO_2

diffusion in tobacco leaves grown under long-term drought. *Functional Plant Biology*, **35**, 553-564.

Mori I.C., Rhee J., Shibasaka M., Sasano S., Kaneko T., Horie T. & Katsuhara M. (2014) CO_2 transport by PIP2 aquaporins of barley. *Plant Cell Physiol*, **55**, 251-257.

Mott K.A. (2009) Opinion: stomatal responses to light and CO_2 depend on the mesophyll. *Plant Cell Environ*, **32**, 1479-1486.

Mustilli A.C. (2002) Arabidopsis OST1 Protein Kinase Mediates the Regulation of Stomatal Aperture by Abscisic Acid and Acts Upstream of Reactive Oxygen Species Production. *The Plant Cell*, **14**, 3089-3099.

Nafziger E.D. & Koller H.R. (1976) Influence of leaf starch concentration on CO_2 assimilation in soybean. *Plant Physiol*, **57**, 560-563.

Negi J., Matsuda O., Nagasawa T., Oba Y., Takahashi H., Kawai-Yamada M., Uchimiya H., Hashimoto M. & Iba K. (2008) CO_2 regulator SLAC1 and its homologues are essential for anion homeostasis in plant cells. *Nature*, **452**, 483-486.

Nobel P.S. (1977) Internal leaf area and cellular CO_2 resistance: photosynthetic implications of variations with growth conditions and plant species. *Physiologia Plantarum*, **40**, 137-144.

Ogunkanmi A.B., Tucker D.J. & Mansfield T.A. (1973) An improved bio-assay for abscisic acid and other antitranspirants. *New Phytol*, **72**, 277-282.

Otto B., Uehlein N., Sdorra S., Fischer M., Ayaz M., Belastegui-Macadam X., Heckwolf M., Lachnit M., Pede N., Priem N., Reinhard A., Siegfart S., Urban M. & Kaldenhoff R. (2010) Aquaporin tetramer composition modifies the function of tobacco aquaporins. *J Biol Chem*, **285**, 31253-31260.

Pantin F., Monnet F., Jannaud D., Costa J.M., Renaud J., Muller B., Simonneau T. & Genty B. (2013) The dual effect of abscisic acid on stomata. *New Phytol*, **197**, 65-72.

Parkhurst D.F. & Mott K.A. (1990) Intercellular Diffusion Limits to CO_2 Uptake in Leaves Studies in Air and Helox. *Plant Physiol*, **94**, 1024-1032.

Perez-Martin A., Michelazzo C., Torres-Ruiz J.M., Flexas J., Fernandez J.E., Sebastiani L. & Diaz-Espejo A. (2014) Regulation of photosynthesis and stomatal and mesophyll conductance under water stress and recovery in olive trees: correlation with gene expression of carbonic anhydrase and aquaporins. *J Exp Bot*, **65**, 3143-3156.

Pons T.L., Flexas J., von Caemmerer S., Evans J.R., Genty B., Ribas-Carbo M. & Brugnoli E. (2009) Estimating mesophyll conductance to CO_2: methodology, potential errors, and recommendations. *J Exp Bot*, **60**, 2217-2234.

Pou A., Medrano H., Flexas J. & Tyerman S.D. (2013) A putative role for TIP and PIP aquaporins in dynamics of leaf hydraulic and stomatal conductances in grapevine under water stress and re-watering. *Plant Cell Environ*, **36**, 828-843.

Prado K., Boursiac Y., Tournaire-Roux C., Monneuse J.M., Postaire O., Da Ines O., Schaffner A.R., Hem S., Santoni V. & Maurel C. (2013) Regulation of Arabidopsis leaf hydraulics involves light-dependent phosphorylation of aquaporins in veins. *Plant Cell*, **25**, 1029-1039.

Prak S., Hem S., Boudet J., Viennois G., Sommerer N., Rossignol M., Maurel C. & Santoni V. (2008) Multiple phosphorylations in the C-terminal tail of plant plasma membrane aquaporins role in subcellular trafficking of AtPIP2; 1 in response to salt stress. *Molecular & Cellular Proteomics*, **7**,

1019-1030.

Preston G.M., Carroll T.P., Guggino W.B. & Agre P. (1992) Appearance of water channels in *Xenopus oocytes* expressing red cell CHIP28 protein. *Science*, **256**, 385-387.

Price G.D., von Caemmerer S., Evans J.R., Yu J.-W., Lloyd J., Oja V., Kell P., Harrison K., Gallagher A. & Badger M.R. (1994) Specific reduction of chloroplast carbonic anhydrase activity by antisense RNA in transgenic tobacco plants has a minor effect on photosynthetic CO_2 assimilation. *Planta*, **193**, 331-340.

Sade N., Shatil-Cohen A., Attia Z., Maurel C., Boursiac Y., Kelly G., Granot D., Yaaran A., Lerner S. & Moshelion M. (2014) The role of plasma membrane aquaporins in regulating the bundle sheath-mesophyll continuum and leaf hydraulics. *Plant Physiol*, **166**, 1609-1620.

Seo M. & Koshiba T. (2002) Complex regulation of ABA biosynthesis in plants. *Trends in plant science*, **7**, 41-48 1360-1385.

Sharkey T.D., Bernacchi C.J., Farquhar G.D. & Singsaas E.L. (2007) Fitting photosynthetic carbon dioxide response curves for C_3 leaves. *Plant Cell Environ*, **30**, 1035-1040.

Shatil-Cohen A., Attia Z. & Moshelion M. (2011) Bundle-sheath cell regulation of xylem-mesophyll water transport via aquaporins under drought stress: a target of xylem-borne ABA? *Plant J*, **67**, 72-80.

Shinozaki K. & Yamaguchi-Shinozaki K. (2007) Gene networks involved in drought stress response and tolerance. *J Exp Bot*, **58**, 221-227.

Sims D.A., Seemann J.R. & Luo Y. (1998) The significance of differences in the mechanisms of photosynthetic acclimation to light, nitrogen and CO_2 for return on investment in leaves. *Functional Ecology*, **12**, 185-194.

Singsaas E.L., Ort D.R. & DeLucia E.H. (2004) Elevated CO_2 effects on mesophyll conductance and its consequences for interpreting photosynthetic physiology. *Plant Cell Environ*, **27**, 41-50.

Tardieu F., Zhang J., Katerji N., Bethenod O., Palmer S. & Davies W.J. (1992) Xylem ABA controls the stomatal conductance of field−grown maize subjected to soil compaction or soil drying. *Plant Cell Environ*, **15**, 193-197.

Tazoe Y., von Caemmerer S., Badger M.R. & Evans J.R. (2009) Light and CO_2 do not affect the mesophyll conductance to CO_2 diffusion in wheat leaves. *J Exp Bot*, **60**, 2291-2301.

Tazoe Y., von Caemmerer S., Estavillo G.M. & Evans J.R. (2011) Using tunable diode laser spectroscopy to measure carbon isotope discrimination and mesophyll conductance to CO_2 diffusion dynamically at different CO_2 concentrations. *Plant Cell Environ*, **34**, 580-591.

Terashima I. (1992) Anatomy of non-uniform leaf photosynthesis. *Photosynthesis Research*, **31**, 195-212.

Terashima I., Hanba Y.T., Tazoe Y., Vyas P. & Yano S. (2006) Irradiance and phenotype: comparative eco-development of sun and shade leaves in relation to photosynthetic CO_2 diffusion. *J Exp Bot*, **57**, 343-354.

Terashima I., Hanba Y.T., Tholen D. & Niinemets U. (2011) Leaf functional anatomy in relation to photosynthesis. *Plant Physiol*, **155**, 108-116.

Terashima I. & Ono K. (2002) Effects of $HgCl_2$ on CO_2 dependence of leaf photosynthesis: evidence indicating involvement of aquaporins in CO_2 diffusion across the plasma membrane. *Plant and Cell Physiology*, **43**, 70-78.

Thain J.F. (1983) Curvature correction factors in the measurement of cell surface areas in plant tissues1. *J Exp Bot*, **34**, 87-94.

Tholen D., Boom C., Noguchi K., Ueda S., Katase T. & Terashima I. (2008) The chloroplast avoidance response decreases internal conductance to CO_2 diffusion in Arabidopsis thaliana leaves. *Plant Cell Environ*, **31**, 1688-1700.

Tholen D., Ethier G., Genty B., Pepin S. & Zhu X.G. (2012) Variable mesophyll conductance revisited: theoretical background and experimental implications. *Plant Cell Environ*, **35**, 2087-2103.

Tholen D. & Zhu X.G. (2011) The mechanistic basis of internal conductance: a theoretical analysis of mesophyll cell photosynthesis and CO_2 diffusion. *Plant Physiol*, **156**, 90-105.

Tornroth-Horsefield S., Wang Y., Hedfalk K., Johanson U., Karlsson M., Tajkhorshid E., Neutze R. & Kjellbom P. (2006) Structural mechanism of plant aquaporin gating. *Nature*, **439**, 688-694.

Tournaire-Roux C., Sutka M., Javot H., Gout E., Gerbeau P., Luu D.-T., Bligny R. & Maurel C. (2003a) Cytosolic pH regulates root water transport during anoxic stress through gating of aquaporins. *Nature*, **425**, 393-397.

Tournaire-Roux C., Sutka M., Javot H., Gout E., Gerbeau P., Luu D.T., Bligny R. & Maurel C. (2003b) Cytosolic pH regulates root water transport during anoxic stress through gating of aquaporins. *Nature*, **425**, 393-397.

Uehlein N., Lovisolo C., Siefritz F. & Kaldenhoff R. (2003) The tobacco aquaporin NtAQP1 is a membrane CO_2 pore with physiological functions. *Nature*, **425**, 734-737.

Uehlein N., Sperling H., Heckwolf M. & Kaldenhoff R. (2012) The Arabidopsis

aquaporin PIP1;2 rules cellular CO_2 uptake. *Plant Cell Environ*, **35**, 1077-1083.

Van Wilder V., Miecielica U., Degand H., Derua R., Waelkens E. & Chaumont F. (2008) Maize plasma membrane aquaporins belonging to the PIP1 and PIP2 subgroups are in vivo phosphorylated. *Plant Cell Physiol*, **49**, 1364-1377.

Von Caemmerer S.v. & Farquhar G.D. (1981) Some relationships between the biochemistry of photosynthesis and the gas exchange of leaves. *Planta*, **153**, 376-387.

Vrabl D., Vaskova M., Hronkova M., Flexas J. & Santrucek J. (2009) Mesophyll conductance to CO_2 transport estimated by two independent methods: effect of variable CO_2 concentration and abscisic acid. *J Exp Bot*, **60**, 2315-2323.

Warren C.R. (2004) The photosynthetic limitation posed by internal conductance to CO_2 movement is increased by nutrient supply. *J Exp Bot*, **55**, 2313-2321.

Warren C.R. (2008) Soil water deficits decrease the internal conductance to CO_2 transfer but atmospheric water deficits do not. *J Exp Bot*, **59**, 327-334.

Wilkinson S. & Davies W.J. (1997) Xylem sap pH increase: a drought signal received at the apoplastic face of the guard cell that involves the suppression of saturable abscisic acid uptake by the epidermal symplast. *Plant Physiol*, **113**, 559-573.

Xue S., Hu H., Ries A., Merilo E., Kollist H. & Schroeder J.I. (2011) Central functions of bicarbonate in S-type anion channel activation and OST1 protein kinase in CO_2 signal transduction in guard cell. *EMBO J*, **30**, 1645-1658.

Zelazny E., Borst J.W., Muylaert M., Batoko H., Hemminga M.A. & Chaumont F. (2007) FRET imaging in living maize cells reveals that plasma membrane aquaporins interact to regulate their subcellular localization. *Proc Natl Acad Sci U S A*, **104**, 12359-12364.